Phenomenological model of the magnetic states of ferromagnetic film with competing surface and bulk anisotropies

A. P. Popov,[1] N. V. Skorodumova,[2] and O. Eriksson[2]
[1]*Moscow Engineering Physics Institute (State University), Kashirskoe Shosse 31, 115409 Moscow, Russia*
[2]*Condensed Matter Theory Group, Department of Physics, Uppsala University, P.O. Box 530, S-75121 Uppsala, Sweden*
(Received 26 July 2007; published 14 January 2008)

The magnetic properties of a film with competing surface and bulk anisotropies and nonuniform ferromagnetic exchange interaction between atomic layers in the surface region have been investigated. The analytic expressions for the criteria of stability of the perpendicular and in-plane states of a film of arbitrary thickness have been derived in the framework of the layer by layer approach. We find that in films characterized by an arbitrary layer-dependent ferromagnetic exchange interaction between atomic layers and layer-dependent anisotropy constants, a canted noncollinear magnetic state becomes favorable when neither the perpendicular nor in-plane state is stable. We construct the diagram of the magnetic states of such a film and analyze the behavior of the magnetic state depending on film thickness. The developed theory can be applied to describe a wide class of quasi-two-dimensional magnetic systems demonstrating phase transitions between collinear and noncollinear magnetic states. In particular, we use this theory to describe the two-step spin-reorientation transition observed in bare Co/Au films.

DOI: 10.1103/PhysRevB.77.014415 PACS number(s): 75.70.Ak

I. INTRODUCTION AND DESCRIPTION OF THE THEORETICAL MODEL

Phase transitions are a common phenomenon encountered in nearly every branch of physics.[1] Modeling the driving forces and the order of the transition often leads to a deeper understanding of the underlying physical processes involved. Magnetism is a rich field in this regard due to the vector nature of the order parameter. Integral to this is the concept of magnetic anisotropy, i.e., the difference in energy for various orientations of the magnetization with respect to a sample. The anisotropy plays a role in every magnetic device.[2,3] Understanding of spin reorientation transitions (SRTs) driven by the change in a balance between the surface, bulk, and shape anisotropy with film thickness or with temperature is an important source of knowledge regarding magnetic anisotropy. This information is invaluable because *ab initio* calculations in even the simplest systems are difficult, and it is currently not feasible to predict, from first principles, the behavior of complicated alloys and multilayered systems at finite temperatures.

During the past several decades, considerable attention has been paid to the experimental and theoretical investigation of ultrathin bare Fe, Co, and Ni films deposited on Au, Ag, Cu, and Pd substrata.[4–6] The obtained results are summarized in the recent comprehensive review of Ref. 6. This interest is triggered by the occurrence of novel magnetic structures and phenomena in ultrathin films, which have no counterparts in the respective bulk systems, and by their possible technological applications.[2,3] Ultrathin magnetic films exhibit highly anisotropic magnetic properties. The magnetic state of an ultrathin film depends on its thickness that substantially enriches thin-film magnetism compared to three-dimensional magnetism. One of the most interesting phenomena occurring in thin magnetic films is the SRT with film thickness. The polar SRT between the perpendicular and in-plane magnetic directions $m_\perp \rightarrow m_\parallel$ with increasing film thickness N has been discovered in Fe/Cu(001),[7,8] Fe/Ag(001),[9–12] Co/Au(111) (Refs. 13–18) films. In contrast, Ni/Cu(001) films exhibit the *reversed* polar SRT, from the in-plane to perpendicular orientation, $m_\parallel \rightarrow m_\perp$, with increasing film thickness.[19–21]

The present work is devoted to the theoretical description of the polar SRT $m_\perp \rightarrow m_\parallel$ in bare Co/Au films with film thickness in the framework of a simple phenomenological model. The description of this phenomenon requires a model that would *adequately* describe the magnetic properties of Co/Au films. However, in the predominant majority of published papers, the experimental data are compared with the solution of the following inadequate primitive model for the energy of the magnetic anisotropy of a thin film:

$$E_{anis} = K_B \sin^2 \theta + \frac{K_S}{d} \sin^2 \theta. \tag{1}$$

Here, K_B and K_S are bulk and surface anisotropy constants, respectively. The magnitudes of these constants are to be obtained from the comparison of the theoretical results and experimental data. θ is an angle between the magnetization vector and the film plane and d is the film thickness. There are two principal mechanisms, which could explain the perpendicular anisotropy in thin Co/Au films. The first is the broken symmetry of Co atoms at the Co film surface and the Co-Au interface,[22] and the second involves the magnetoelastic properties of the Co-Au interfacial alloy.[23] At present, it is well established that interfacial alloying is the dominant mechanism.[23] Bearing this in mind in Eq. (1), we take into account the surface anisotropy only at one side of the film, namely, at the interface.

Treating the SRT $m_\perp \rightarrow m_\parallel$ within the model described by Eq. (1), one makes the assumption about a *direct* competition between the interface anisotropy energy that favors the perpendicular orientation $m_\perp$ ($K_S < 0$) and the bulk anisotropy energy that favors the in-plane orientation $m_\parallel$ ($K_B > 0$). If the film thickness d is small, then the interface anisotropy energy dominates and, thus, the film is in the perpendicular state. An

increase in film thickness leads to an increase in the bulk contribution to the anisotropy energy, eventually leading to the occurrence of the SRT to the in-plane state. The treatment of the SRT within model (1) is based on the assumption that the energy of the exchange interaction between atomic layers is infinitely large. Because of that, the magnetization vectors of all the atomic layers are parallel to each other and characterized by a single orientation angle θ. In this limiting case, the terms describing the exchange interaction between neighbor atomic layers do not depend on the orientation angle; consequently, they are not taken into account in the model (1). If the exchange interaction has a finite magnitude at least between the interface and the next atomic layers, the orientation of the magnetization vector of the surface layer is determined by the competition between the surface anisotropy energy and the exchange interaction between surface and subsurface layers rather than by the competition between surface and bulk anisotropy energies. Hence, in the case of a finite exchange interaction, the assumption about the direct competition between surface and bulk anisotropy energies is not quite correct.

There are only two stable solutions in the model (1): perpendicular $m_\perp$ and in-plane $m_\parallel$. As a consequence, the SRT $m_\perp \rightarrow m_\parallel$ described by model (1) is discontinuous. The nature of polar SRT with thickness in Co/Au films has been investigated in Ref. 13 where the authors answered the question whether the out-of-plane remanence decrease is due to a breakup into domains or rather due to a rotation of magnetization from the out-of-plane toward the in-plane orientation. Monitoring the magnetization direction in a domain allowed the authors of Ref. 13 to unequivocally conclude that the magnetization crossover took place by a continuous rotation. This experimental result has never been argued.[24] However, a more recent experimental work[16] provides some evidence of phase coexistence that is characteristic of a discontinuous first-order SRT. At the same time, in Ref. 17, the same authors demonstrate that in the vicinity of the SRT with film thickness the magnetic susceptibility exhibits an asymmetrical peak that is characteristic of a continuous second-order SRT.[25] Therefore, the analysis of the available experimental data allows us to conclude that the results reporting on the continuous SRT $m_\perp \rightarrow m_\parallel$ with Co film thickness appear to be more convincing.

So far, a common approach to the description of the continuous SRT $m_\perp \rightarrow m_\parallel$ within model (1) was to include the quadratic contribution to the anisotropy energy $K_{B2} \sin^4 \theta$ into Eq. (1).[6] This term determines the width of the SRT $m_\perp \rightarrow m_\parallel$. Similar to K_B and K_S, the anisotropy constant K_{B2} is to be determined from the comparison of experiment and theory. Over the past decade, a considerable effort has been spent trying to find grounds for the presence of the effective high-order anisotropies like $K_{B2} \sin^4 \theta$ in the expression for the anisotropy energy [Eq. (1)] (read, for example, items 1–3 on pp. 156 and 157 and Sec. IV in the recent comprehensive review in Ref. 6 and references therein). A variety of mechanisms able to give rise to the effective high-order anisotropies, which have no counterpart in the underlying Hamiltonian, have been proposed. In particular, it has been suggested that the roughness and nonuniformity of a film can lead to the appearance of high-order anisotropies. In the present work, we demonstrate that when the exchange interaction between atomic layers is finite, the continuous SRT $m_\perp \rightarrow m_\parallel$ with film thickness can be described without involving high-order anisotropies. This finding is in agreement with the results of previous theoretical works.[26,27] We do not claim that the higher order anisotropies are absent in Co/Au films or in other multilayer systems. We just demonstrate that the description of SRT with film thickness in the case of Co/Au films *does not* require higher order anisotropies. Because of that, we follow the well-known and commonly accepted rule that the phenomenological description of a physical phenomenon should be performed with the minimal possible number of adjustable parameters. Hence, in our description of SRT in Co/Au films, we take into account only the anisotropy constants of the lowest order.

Due to the infinite magnitude of the exchange interaction assumed in model (1), the magnetization vector of all layers are parallel to each other; thus, all of them are characterized by a single orientation angle θ. Such an approach is well justified when one wants to describe the magnetic properties of Fe and Ni films as in these metals the domain wall width is equal to 138 and 238 lattice parameters, respectively,[28] that is, much larger than the film thickness (approximately ten atomic layers). In this limit, during the SRT the film behaves as one entity, as a giant magnetic molecule; therefore, the single-domain picture is quite adequate. In contrast, in Co the domain wall width is only about 30 lattice parameters,[28] that is, comparable with the film thickness. Besides, in Co films the shape anisotropy and bulk anisotropy act in the same direction, both prompting the magnetization vector to orient in plane. It means that in a thin Co film, the domain wall width must be even smaller than in bulk Co samples. Because of these reasons, the continuous SRT $m_\perp \rightarrow m_\parallel$ in a Co film has to go via an intermediate canted noncollinear state, $m_\angle$, rather than via the canted collinear state. This statement is proven in Sec. II of the present paper where we show that a canted noncollinear state is more energetically favorable than the in-plane, perpendicular, and canted collinear states. Therefore, we conclude that even with account of the term $K_{B2} \sin^4 \theta$, the model (1) cannot adequately describe the magnetic properties of Co films. The canted noncollinear state is a part of the domain wall with a layer-dependent orientation angle. The possibility for such a ground-state noncollinear spin configuration to exist in a semi-infinite ferromagnetic sample was first noted in Ref. 29 and in thin films in Ref. 30.

To describe the canted noncollinear state, one should use the model expression for thermodynamic potential, taking into account the finite magnitude of the exchange interaction between atomic layers,

$$\Phi = -J_{SB} M_S M_B \cos(\theta_1 - \theta_2) - J_{BB} M_B^2 \sum_{n=2}^{N-1} \cos(\theta_n - \theta_{n+1}) + K_S M_S^2 \sin^2 \theta_1 + K_B M_B^2 \sum_{n=2}^{N} \sin^2 \theta_n. \quad (2)$$

Applying model (1) for the restoration of the anisotropy constants K_S and K_B from the comparison of theory and experi-

ment, one makes the assumption that these constants are small (compared to the infinite magnitude of the exchange interaction). Obviously, it is not entirely correct to make such an assumption about K_S and K_B, whose values are yet to be determined. In model (2), terms describing the exchange interaction between atomic layers (J_{SB} and J_{BB}) are taken into account explicitly; i.e., no initial assumptions are made about the magnitude of anisotropy constants K_S and K_B. Generally, in magnetic materials, such as Fe and Ni, the anisotropy energy is much smaller than the energy of the exchange interaction. However, as it has been mentioned in Ref. 6 (p. 194), it does not mean that the case where the anisotropy energy is comparable with the energy of the exchange interaction is a mere physical abstraction. For example, in multilayer films with alternating magnetic and nonmagnetic layers, the exchange interaction between neighbor magnetic layers can be substantially diminished, increasing the thickness of nonmagnetic layers, and it can become comparable with the anisotropy energy. Therefore, a proper investigation of model (2) could be useful not only for the description of the SRT $m_\perp \rightarrow m_\parallel$ with thickness observed in Co films, but also for a much wider class of magnetic systems demonstrating the collinear-to-noncollinear SRT.[6]

Model (2) is the simplest model that is able to describe a canted noncollinear state, but even for this simple model there exist no analytic results. Moreover, some authors state that in the discrete model [Eq. (2)], no analytic results can be obtained.[33] The lack of analytical results strongly complicates the procedure of getting information about the anisotropy energy of thin films, multilayers, and sandwiches by comparing theory and experiment. In particular, there is no analytic expression for the stability criterion of the perpendicular and in-plane states for a film of arbitrary thickness N. The canted noncollinear state has been shown to be favorable only for the uniform exchange interaction across the film.[26,27] There exist no diagram of magnetic states in the coordinates (K_S, K_B) for films of arbitrary N. The absence of analytic results for model (2) is, however, easy to understand. Despite the simplicity of the physical mechanism driving continuous SRT $m_\perp \rightarrow m_\parallel$, its description comes across difficulties related to the analyses of the function [Eq. (2)], which depends on many variables, namely, orientation angles $\theta_1, \theta_2, \ldots, \theta_N$. Because of that, the search for the minima of the thermodynamic potential [Eq. (2)] is usually performed within various approximations. For instance, within the continuum approach, the discrete atomic structure of the film is ignored.[29,31–34] Instead of a discrete layer index, the continuous coordinate x is introduced and the magnetization profile is described by the continuous function $\theta(x)$. The continuum approach is applicable only in the case of small anisotropy constants for it is based on the assumption that the change in the orientation of magnetization vector with a layer index is very small. In order to justify the application of the continuum approach for the description of the magnetic properties of thin films (five to ten atomic layers), the authors of Refs. 32–34 solved the discrete model [Eq. (2)] numerically[33] and compared the results to those obtained in the continuum approach. However, the numerical solution of model (2) for some particular values of model parameters cannot reveal the whole physical picture model (2) can provide. Hence, it cannot serve as an exhaustive proof that the continuum approach is applicable for the description of the magnetic properties of ultrathin films. Moreover, in our previous work,[35] we have shown that the application of the continuum approach leads to a wrong phase diagram even for a semi-infinite ferromagnetic film. On the other hand, in the papers where the discrete layer structure of the film has been taken into account, the results have been obtained either numerically or within the perturbation theory. In the latter case, the deviation of orientation angles from the orientation angle averaged across the film is believed to be small, and it serves as the so-called small parameter.[6,36] However, in the case of a large difference between the surface and bulk anisotropy constants $|K_S| \gg |K_B|$, which is actually often the case, and when the difference between the exchange interaction in the surface region and in bulk is large $J_{SB} \ll J_{BB}$, which is also probable, the deviation of surface magnetization from the average magnetization can appear to be large. Therefore, such an approach cannot provide us with the total physical picture. We notice that the applications of discrete and continuum methods one can find in literature have much in common as within both approaches investigators mainly aimed at finding the magnetization profile of a film. This is not surprising for in the absence of the true diagram of magnetic states, only the magnetization profile can give an information about the magnetic state of the film.

References 26 and 27 stand out in the field of the theoretical description of a continuous SRT $m_\perp \rightarrow m_\parallel$ with film thickness. The authors of these papers use the discrete approach and solve a model similar to model (2). They have obtained theoretical results similar to those reported in the present work: (A) The SRT $m_\perp \rightarrow m_\parallel$ with film thickness is realized via an intermediate canted noncollinear state $m_\angle$. (B) The SRT $m_\perp \rightarrow m_\parallel$ with film thickness can be described without taking into account the high order anisotropies in the expansion of anisotropy energy.

Since the used approaches and the results obtained in Refs. 26 and 27 are very close to those achieved in the present work, it is worth comparing the methods applied in both cases in more detail. In Ref. 26, the diagrams of magnetic states $m_\parallel$, $m_\perp$, and $m_\angle$ in coordinates λ_1, λ_2 for $N=2,3,4,5$ were constructed for a Co film described within a model similar to model (2). λ_1 and λ_2 are anisotropy constants of two surfaces of the film. We note that in Ref. 26, the analytic results (the equations determining lines that confine the regions corresponding to $m_\parallel$, $m_\perp$, and $m_\angle$ states) were presented only for the case of a bilayer $N=2$. The authors of Ref. 26 promised to present the derivation of the criterion of stability of the in-plane and perpendicular states in the future. However, even for the case of a bilayer, this derivation has never been published.[37] We note that in Ref. 26 all the results were obtained in the assumption that the exchange interaction between atomic layers is not dependent on the layer index. At the same time, in the surface region, the exchange interaction and the magnetic moment are most likely different from those in the layers far from the interface. Moreover, in Ref. 26, all bulk anisotropy constants were set to zero. To justify this approximation, the authors cited Refs. 38 and 39, where surface and bulk anisotropy constants of Fe/Cu and Fe/Au films had been obtained in

first-principles calculations. However, the authors of Ref. 26 applied their theory exceptionally for the description of the SRT in Co/Au film; hence, citing Refs. 38 and 39 is irrelevant. In the later work by the same authors,[27] the theory was generalized for the case of finite temperature. Despite the statement made in the concluding part of this paper, that they "derived explicit expressions for the boundaries of the regions related to normal-to-plane, canted, and in-plane ground states in the corresponding parameter space" one cannot find any explicit expressions for $N>2$ in their paper.[27] Fortunately, the approximations used by the authors of Refs. 26 and 27 did not prevent them from getting the right physical conclusions (A) and (B) (read above). However, the absence of formulas for the stability criterion of the in-plane and perpendicular states for an arbitrary N makes it impossible to get information about the energy of magnetic anisotropy by comparing theory and experimental results. The main goal of the present work is to fill this gap in the theory of thin-film magnetism. In particular, here, we present the analytic expressions for the criterion of stability of the in-plane and perpendicular states and construct the diagram of the magnetic states of a finite magnetic film in coordinates K_S, K_B.

It is convenient to work with the reduced expression for the model thermodynamic potential,

$$\varphi = \frac{\Phi}{J_{BB}M_B^2} = -\gamma\cos(\theta_1 - \theta_2) - \sum_{n=2}^{N-1}\cos(\theta_n - \theta_{n+1}) + \frac{\gamma k_S}{2}\sin^2\theta_1 + \frac{k_B}{2}\sum_{n=2}^{N}\sin^2\theta_n. \quad (3)$$

The reduced surface anisotropy constant k_S related to the Co-Au interface, the bulk anisotropy constant of all other atomic layers in the Co film, k_B, and the parameter γ, characterizing the nonuniformity of the exchange interaction in the vicinity of the Co-Au interface, are given by the following formulas:

$$k_S = \frac{2K_S M_S^2}{J_{SB}M_S M_B}, \quad k_B = \frac{2K_B M_B^2}{J_{BB}M_B^2}, \quad \gamma = \frac{J_{SB}M_S M_B}{J_{BB}M_B^2}. \quad (4)$$

The main goals of the present work are the following.

(I) To prove that within model (3) a canted noncollinear state is most favorable compared to perpendicular, in-plane, and canted collinear states in the case of an arbitrary nonuniformity of the ferromagnetic exchange interaction across the film of a finite thickness N. A canted noncollinear state occurs when neither perpendicular nor in-plane states are stable.

(II) To derive the analytic expression for the criterion of stability of the perpendicular ($m_\perp$) and in-plane ($m_\parallel$) magnetic states of a ferromagnetic film of finite N, described by model (3), taking into account the discrete layer structure of the film as well as the nonuniform exchange interaction across the film. We also analyze these expressions in the limiting case of small anisotropy constants.

(III) To construct the diagram of the magnetic states of a thin film in coordinates (γ, k_S, k_B) for chosen N. To compare this diagram with the diagram of the magnetic states of a semi-infinite ferromagnetic sample obtained in our previous work.[35,43] To investigate the dependence of the diagram on the parameter γ, characterizing the nonuniform exchange interaction in the surface region of the film.

(IV) To construct the diagram of the magnetic states in coordinates (k_S, k_B) for a chosen parameter γ and various N. To describe the SRT $m_\perp \rightarrow m_\parallel$ with film thickness N via the intermediate canted noncollinear state $m_\angle$.

In the present work we solve model (2) and demonstrate its applicability for the description of the SRT $m_\perp \rightarrow m_\parallel$ in Co/Au films. Because of that, we have to note that in accordance with experimental data, the as-grown Co ultrathin films consist of domains with the opposite orientations of magnetization that is perpendicular to the film plane. In the vicinity of the SRT, the size of domains decreases with thickness.[13–18] The multidomain magnetic state of the films as well as the decrease of the domain size with film thickness was investigated in detail in theoretical works.[40–45] In particular, it has been shown that the energy difference between the multidomain state and the single-domain state is very small, and these states are separated from each other by an energy barrier. Within model (3) used in the present work, we restrict ourselves by considering the magnetic states of the film to be uniform in the plane of the film and taking into account the nonuniform state only across the film, i.e., canted noncollinear state. This approach is quite justified as it has been shown experimentally that Co films can be transformed into a single-domain state by magnetic field.[14,15] In particular, in Ref. 15 it has been demonstrated that on magnetizing Co films in an external field, the magnetic microstructure can be transformed into a metastable single-domain state with the perpendicular magnetization. The transition into the in-plane magnetization state is shifted to even higher thicknesses, and a continuous rotation of the magnetization from the vertical to the in-plane orientation was observed. This single-domain configuration with the perpendicular magnetization could not be changed by further demagnetization procedures. Heating the sample reestablished qualitatively the same domain structure as before when applying the field. Therefore, the investigation of the SRT $m_\perp \rightarrow m_\parallel$ with film thickness within model (3), in fact, means the investigation of the SRT between metastable single-domain states $m_\perp$ and $m_\parallel$ obtained on magnetizing Co film in external field.

The angle dependence of the shape anisotropy inside each atomic layer is the same as the angle dependence of magnetocrystalline anisotropy. Therefore, we assume that the contribution of the shape anisotropy is already included in terms describing the anisotropy energy in model (2). The contribution of the shape anisotropy to the exchange interaction between neighbor layers is relatively small. Therefore, we assume that it is already accounted for in model (2) by small renormalization of exchange interactions between atomic layers. The magnitude and properties of the shape anisotropy for uniform films with various crystal structures and orientations are well known. The matrix elements of the magnetodipole interaction Φ_{pq} are presented in Ref. 36. For the sake of compactness of formulas, the contribution of the shape anisotropy is not written explicitly in model (2). The mathematical method used in the present work is based on the analysis of the sign of the quadratic form, resulting from the

expansion of thermodynamic potential to the second order of every orientation angle. In turn, this analysis is based on the analysis of a square three-diagonal matrix that describes this quadratic form. Since matrix Φ_{pq} which describes magnetodipole interaction, is also square and three diagonal, the analysis of the ground state of a film described by model (2) presented here can be repeated, explicitly taking into account the shape anisotropy. That is why the absence of the account of the magnetodipole interaction in an explicit form in model (2) simplifies the formulas rather than the physical picture.

In the present work, we do not consider the microscopic origin of the interface and bulk anisotropy. Neither do we discuss the applicability of the Heisenberg model for the treatment of magnetic properties of the Co film that is a transition metal with itinerant d electrons. These problems have been discussed in detail in the recent review[6] (Appendix A, Sec. A 1, and Sec. A 3), and we share the viewpoint of the authors of Ref. 6.

The present paper is organized in the following way. In Sec. II, the energy of the canted noncollinear state is compared with the energy of the perpendicular and in-plane states. In Sec. III, we demonstrate that in the parameter space (γ, k_S, k_B), there is a region where the perpendicular state and the in-plane state are unstable. In Sec. IV, the evolution of borders in the (k_S, k_B) diagram between regions corresponding to different magnetic states of a film on film thickness is investigated. Also, in Sec. IV, the description of the SRT $m_\perp \rightarrow m_\parallel$ observed in a bare Co/Au film with film thickness is presented. In Sec. V, we consider the theory presented in the limiting case of a very small bulk anisotropy constant. In Sec. VI, an analytic solution of the problem of a bilayer with competing anisotropies at both sides of a film is presented. The derivation of the stability criterion of the perpendicular state of a film is presented in Appendix A. The derivation of the criterion of stability of the in-plane state of a film is presented in Appendix B.

II. COMPARISON OF THE ENERGIES OF CANTED NONCOLLINEAR, IN-PLANE, AND PERPENDICULAR STATES

In the present work, the continuous SRT $m_\perp \rightarrow m_\parallel$ with film thickness is treated as a transition via an intermediate canted noncollinear state $m_\angle$. Because of that, it is important to prove that this state is energetically favorable compared to both the in-plane and perpendicular states. This task has been considered in Ref. 27 for the particular case of the uniform exchange interaction across the film. In the present work, the difference between the exchange interaction in the surface region and in bulk layers is taken into account. Therefore, we compare the energies of $m_\angle$, $m_\perp$, and $m_\parallel$ states in the general case: $\gamma \neq 1$. As a matter of fact, we go slightly further and generalize model (3) for the case of an arbitrary nonuniform exchange interaction across the film. In other words, the reduced exchange interaction between nth and $(n+1)$th layers $\gamma_{n,n+1} \equiv \gamma_n > 0$ is supposed to be layer dependent across the entire film rather than only in the surface region. The anisotropy constant of each atomic layer, k_n, can have any sign, and it is assumed to be also a layer-dependent parameter. Then, model (3) can be rewritten as

$$\varphi = -\sum_{n=1}^{N-1} \gamma_n \cos(\theta_n - \theta_{n+1}) + \frac{1}{2}\sum_{n=1}^{N} k_n \sin^2 \theta_n. \tag{5}$$

The minimization of the thermodynamic potential [Eq. (5)] with respect to each orientation angle θ_n gives a set of N equations,

$$\gamma_1 \sin(\theta_1 - \theta_2) + k_1 \sin\theta_1 \cos\theta_1 = 0,$$

$$-\gamma_1 \sin(\theta_1 - \theta_2) + \gamma_2 \sin(\theta_2 - \theta_3) + k_2 \sin\theta_2 \cos\theta_2 = 0,$$

$$\cdots$$

$$-\gamma_{n-1} \sin(\theta_{n-1} - \theta_n) + \gamma_n \sin(\theta_n - \theta_{n+1}) + k_n \sin\theta_n \cos\theta_n = 0,$$

$$\cdots$$

$$-\gamma_{N-2} \sin(\theta_{N-2} - \theta_{N-1}) + \gamma_{N-1} \sin(\theta_{N-1} - \theta_N) + k_{N-1} \sin\theta_{N-1} \cos\theta_{N-1} = 0,$$

$$-\gamma_{N-1} \sin(\theta_{N-1} - \theta_N) + k_N \sin\theta_N \cos\theta_N = 0. \tag{6}$$

Formally, the orientation angles θ_n can have any values. However, following the set of Eq. (6), if the set of orientation angles $\{\theta_n\}$ corresponding to a canted noncollinear state satisfies this system of equations, then the following sets of orientation angles $\{-\theta_n\}$, $\{\pi - \theta_n\}$, and $\{\theta_n + \pi\}$ satisfy this system of equations as well. All these solutions correspond to the same energy. This symmetry of nontrivial solutions allows one to restrict the search for nontrivial solutions to the interval $\theta_n \in [0, \pi/2]$. In accordance with this choice, we believe that the parallel and perpendicular states of a film correspond to solutions $\{\theta_n = 0\}$ and $\{\theta_n = \pi/2\}$ rather than to solutions $\{\theta_n = \pi\}$ and $\{\theta_n = -\pi/2\}$, for example. By the same reason, we believe that $\theta_n = 0$ and $\theta_n = \pi/2$ are boundary values for the considered interval $\theta_n \in [0, \pi/2]$. Also, we have to mention that $\{\theta_n = 0\}$ and $\{\theta_n = \pi/2\}$ satisfy the set of Eq. (6) for any magnitudes of model parameters.

Instead of solving these equations with respect to orientation angles θ_n, we fix the configuration corresponding to the canted noncollinear state $\theta_1, \theta_2, \ldots, \theta_N$ and express the reduced anisotropy constants k_n from the corresponding equations in Eq. (6). The substitution of k_n in Eq. (5) by the corresponding expression leads to the following expression for the thermodynamic potential of a canted noncollinear state $m_\angle$,

$$\varphi_\angle = -\frac{1}{2}\sum_{n=1}^{N-1} \gamma_n \left(\frac{\cos\theta_{n+1}}{\cos\theta_n} + \frac{\cos\theta_n}{\cos\theta_{n+1}} \right). \tag{7}$$

The expressions for the thermodynamic potential of the in-plane state $m_\parallel (\theta_1 = 0, \theta_2 = 0, \ldots, \theta_N = 0)$ and the perpendicular state $m_\perp (\theta_1 = \pi/2, \theta_2 = \pi/2, \ldots, \theta_N = \pi/2)$ follow from Eq. (5) and are given by formulas

$$\varphi_\parallel = -\sum_{n=1}^{N-1} \gamma_n, \tag{8}$$

$$\varphi_{\perp} = -\sum_{n=1}^{N-1} \gamma_n + \frac{1}{2}\sum_{n=1}^{N} k_n. \quad (9)$$

After some algebra, the expressions for differences $\varphi_{\parallel} - \varphi_{\angle}$ and $\varphi_{\perp} - \varphi_{\angle}$ can be written in the following form:

$$\varphi_{\parallel} - \varphi_{\angle} = \frac{1}{2}\sum_{n=1}^{N-1} \gamma_n \left(\frac{\cos\theta_{n+1}}{\cos\theta_n} - 2 + \frac{\cos\theta_n}{\cos\theta_{n+1}} \right) \geqslant 0, \quad (10)$$

$$\varphi_{\perp} - \varphi_{\angle} = \frac{1}{2}\sum_{n=1}^{N-1} \gamma_n \left(\frac{\sin\theta_{n+1}}{\sin\theta_n} - 2 + \frac{\sin\theta_n}{\sin\theta_{n+1}} \right) \geqslant 0. \quad (11)$$

It follows from Eqs. (10) and (11) that since $\gamma_n > 0$ the canted noncollinear state is always favorable compared to both the in-plane state and the perpendicular state. In the vicinity of the SRT $m_{\angle} \to m_{\parallel}$, all orientation angles θ_n approach zero and the ratio of cosines approaches 1. As a consequence, inequality (10) transforms into equality. Similar to this, in the vicinity of SRT $m_{\angle} \to m_{\perp}$ all orientation angles θ_n approach $\pi/2$ and the ratio of sinuses approaches 1; thus, inequality (11) transforms into equality. The canted noncollinear state is realized when the in-plane state and the perpendicular state are no longer stable. In the next sections, it will be demonstrated that in the parameter space (γ, k_S, k_B), there is a region where neither the in-plane nor the perpendicular state is stable. In Sec. VI, for the particular case of the bilayer it will be demonstrated that the canted noncollinear state cannot realize in the regions where the perpendicular and in-plane states are stable.

As for the canted collinear state, we can note that, first, in the N-dimensional space the point corresponding to the canted collinear state $\theta_1 = \theta_2 = \theta_3 = \cdots = \theta_N \equiv \theta, 0 < \theta < \pi/2$ does not satisfy the set of Eq. (6). It means that this point does not satisfy the necessary condition for the extremum of the thermodynamic potential [Eq. (5)]. Second, in the N-dimensional space, the point $(\theta, \theta, \ldots, \theta)$ is an inner point in the region $0 < \theta_n < \pi/2, n = 1, 2, \ldots, N$; i.e., it does not belong to the border of this region. Therefore, the canted collinear state cannot correspond to a minimum of the thermodynamic potential [Eq. (5)]. Based on the performed analysis, we conclude that the continuous SRT $m_{\perp} \to m_{\parallel}$ with film thickness goes via an intermediate canted noncollinear state.

III. DIAGRAM OF THE MAGNETIC STATES OF A FILM OF FINITE THICKNESS IN COORDINATES (γ, k_S, k_B)

In this section, we demonstrate that for a film of finite thickness there is a region in the three-dimensional space (γ, k_S, k_B) where neither the perpendicular state nor the in-plane state is stable. In accordance with the results of the previous section, it means that this region corresponds to the canted noncollinear state. Also, we discuss the qualitative difference between the diagrams of the magnetic states of a finite film and a semi-infinite sample.

The diagrams of the magnetic states of a bilayer ($N=2$) and a trilayer ($N=3$) in coordinates (γ, k_S, k_B) are presented in Figs. 1 and 2. These diagrams are constructed based on the analytic expressions for the stability criteria of the perpendicular and in-plane states obtained for arbitrary N (see Appendixes A and B). The diagram for a semi-infinite ferromagnetic sample in coordinates (γ, k_S, k_B) is presented in Fig. 3. This diagram is constructed using the stability criteria obtained in our previous works.[35,46] These criteria are special cases of the general criteria obtained in the present work. They follow from formulas (A22), (A26), (B3), and (B5) in the limiting case $N \to \infty$. The stability criteria for semi-infinite ferromagnetic samples have already been used for the description of a continuous SRT $m_{\parallel} \to m_{\angle}$ with temperature,[47] discovered in ultrathin Fe films deposited on a thick Gd(0001) film.[48,49] These criteria have also been used in the study of the layer-dependent magnetic susceptibility in the surface region of a nonuniform semi-infinite ferromagnetic.[45]

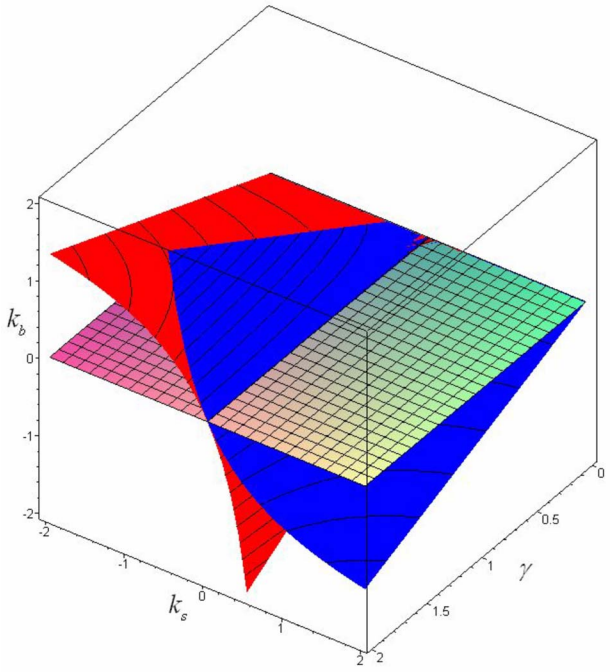

FIG. 1. (Color online) Diagram of magnetic states of a bilayer $N=2$. The perpendicular state exists only for $k_S < 1$. The region corresponding to the perpendicular state is situated below the red surface. The plane asymptote $k_S = 1$ for the red surface is not shown. The in-plane state exists only for $k_S > -1$. The region corresponding to the in-plane state lies above the blue surface. The plane asymptote $k_S = -1$ for the blue surface is not shown. The region corresponding to the canted noncollinear state is situated above the red surface and below the blue surface for $-1 < k_S < +1$, above the red surface for $k_S < -1$, and below the blue surface for $k_S > +1$. The horizontal plane $k_B = 0$ serves to guide the eye.

The diagrams of magnetic states for $N=2$ (Fig. 1) and $N=3$ (Fig. 3) have two asymptotes, two planes: $k_S = -1$ for the red surface and $k_S = +1$ for the blue surface. To avoid the overloading of Figs. 2 and 3, we do not show the plane asymptotes in these figures. In these diagrams, the region corresponding to the perpendicular state exists only for $k_S < 1$, and it is situated below the red surface; the region cor-

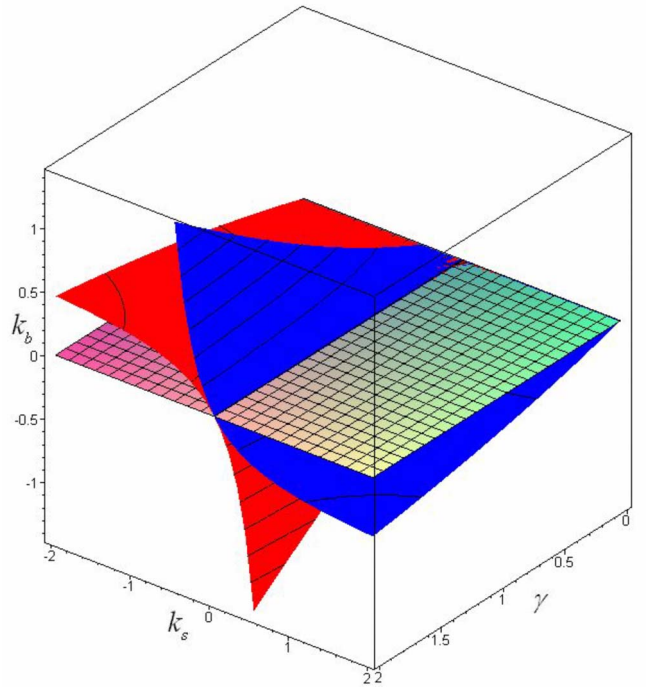

FIG. 2. (Color online) Diagram of magnetic states of a three-layer film $N=3$. The perpendicular state exists only for $k_S<1$. The region corresponding to the perpendicular state is situated below the red surface. The plane asymptote $k_S=1$ for the red surface is not shown. The in-plane state exists only for $k_S>-1$. The region corresponding to the in-plane state lies above the blue surface. The plane asymptote $k_S=-1$ for the blue surface is not shown. The region corresponding to the canted noncollinear state is situated above the red surface and below the blue surface for $-1<k_S<+1$, above the red surface for $k_S<-1$, and below the blue surface for $k_S>+1$. The horizontal plane $k_B=0$ serves to guide the eye.

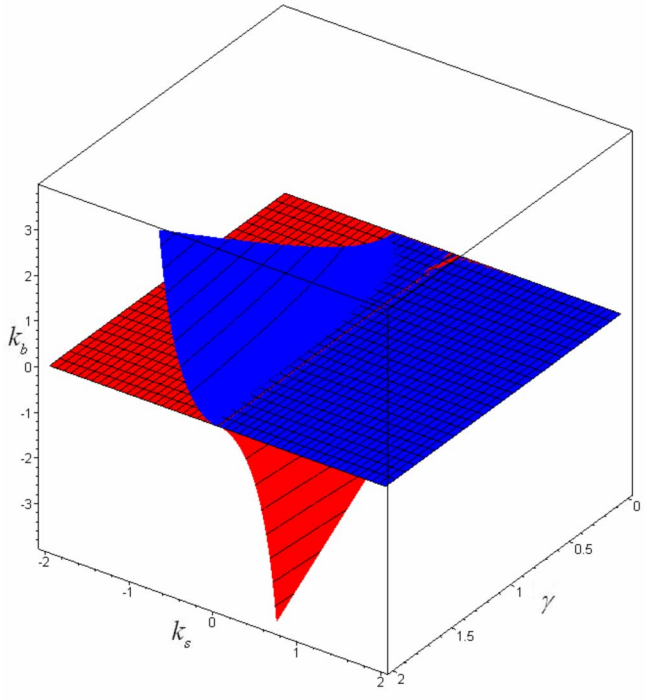

FIG. 3. (Color online) Diagram of magnetic states of a semi-infinite film $N\rightarrow\infty$. The perpendicular state exists only for $k_S<+1$. The region corresponding to the perpendicular state is positioned below the red surface. The plane asymptote $k_S=1$ for the red surface is not shown. The in-plane state exists only for $k_S>-1$. The region corresponding to the in-plane state is positioned above the blue surface. The plane asymptote $k_S=-1$ for the blue surface is not shown. The region corresponding to the canted noncollinear state lies above the red surface and below the blue surface for $-1<k_S<+1$, above the red surface (plane $k_B=0$) for $k_S<-1$, and below the red surface (plane $k_B=0$) for $k_S>+1$.

responding to the in-plane state exists only for $k_S>-1$, and it is situated above the blue surface (Figs. 1 and 2). Therefore, the perpendicular and in-plane regions do not occupy the entire space of the diagram, but in a certain region neither the perpendicular nor the in-plane state is stable. This region is above the red surface and below the blue surface for $-1<k_S<+1$, above the red surface for $k_S<-1$, and below the blue surface for $k_S>+1$.

The diagram of magnetic states of a semi-infinite ferromagnetic sample ($N\rightarrow\infty$) has two asymptotes, two planes: $k_S=-1$ for the red surface and $k_S=+1$ for the blue surface (Fig. 3). To avoid the overloading of Fig. 3, we do not show the plane asymptotes in these figures. The region where the perpendicular state occurs exists only for $k_S<1$, and it is situated below the red plane $k_B=0$ in the left part of the diagram, $k_S<0$, and below the red surface in the right part of the diagram for $0<k_S<1$. The region corresponding to the in-plane state exists only for $k_S>-1$, and it lies above the blue plane $k_B=0$ in the right part of the diagram $k_S>0$ and above the blue surface in the left part of the diagram for $-1<k_S<0$. Therefore, similar to the diagram of magnetic states of a finite film, the perpendicular and in-plane regions do not occupy the entire space, but we find a region corresponding to the canted noncollinear state positioned above the red surface and below the blue surface for $-1<k_S<+1$, above the red plane $k_B=0$ for $k_S<-1$, and below the blue plane $k_B=0$ for $k_S>+1$.

The comparison of the diagram of the magnetic states of a finite film (Figs. 1 and 2) with that for a semi-infinite sample (Fig. 3) shows that in the former case in the left part of the diagram, $k_S<0$, the region corresponding to the perpendicular state spreads above the plane $k_B=0$ and it is bounded from above by the red surface. It means that in finite films, the perpendicular state can exist for $k_S<0, k_B>0$, whereas this is impossible in the semi-infinite case. Similarly, in the right part of the diagram, $k_S>0$, the region corresponding to the in-plane state of the finite film spreads below the plane $k_B=0$, and it is bounded from below by the blue surface. It means that in the films of finite thickness, the in-plane state can exist for $k_S>0, k_B<0$, whereas this is impossible for a semi-infinite sample. These differences make the diagram for a finite film distinct from that for a semi-infinite sample.

The physical meaning of this result is obvious. In the region ($k_S<0, k_B>0$), the surface anisotropy energy and the bulk anisotropy energy favor the perpendicular and in-plane orientations of magnetization, respectively. In other words,

there is a competition between the surface and bulk anisotropy energies. If the number of atomic layers is infinite, then the finite surface anisotropy energy cannot compete with the infinite bulk anisotropy energy. Therefore, in the left part of the diagram ($k_S<0$) for a semi-infinite sample, the region corresponding to the perpendicular state is bounded from above by the plane $k_B=0$. In a finite film, a large enough absolute value of the surface anisotropy energy ($k_S<0$) can overcome the finite magnitude of the bulk anisotropy energy; thus, the perpendicular state can take place. The region positioned in the left part of the diagrams in Figs. 1 and 2 above the plane $k_B=0$ and below the red surface shrinks with increasing N. One can see this from the comparison of the diagrams for $N=2$ (Fig. 1) and $N=3$ (Fig. 2). In the limiting case $N\to\infty$, this region totally disappears (Fig. 3). Hence, for a semi-infinite sample with $k_S<0$, the perpendicular state can take place only if $k_B<0$. Thus, in the case $k_S<0, k_B>0$, the realization of the perpendicular state in a film is entirely determined by its finite thickness. Similar arguments explain the realization of the in-plane state in the right part, $k_S>0$, of the diagram (Figs. 1 and 2), i.e., above the blue surface and below the horizontal plane $k_B=0$.

It follows from Figs. 1 and 2 that the borders between the regions corresponding to different states shift as the parameter $\gamma>0$ varies. We note, however, that the changes occurring with varying $\gamma>0$ should be considered with care. As it follows from formulas (4) that the reduced surface and bulk anisotropy constants, k_S and k_B, are obtained by dividing the corresponding anisotropy energies by the surface and bulk exchange energy, respectively. This has been done, first, because such a definition of the reduced surface anisotropy constant to some extent simplifies the formal mathematical procedure of the derivation of stability criteria. Second, we have already used this definition in our previous works.[35,43–45] However, the consequence of such a definition of k_S is that the parameter γ becomes a factor in the surface anisotropy energy; i.e., in the third term in Eq. (3), we have $\gamma k_S/2$. Hence, the formal variation of the parameter γ in model (3) means the simultaneous variation of the effective surface anisotropy constant $\tilde{k}_S\equiv\gamma k_S$. This definition of the reduced surface anisotropy constant might not be the best. It is possible to introduce this constant with the same definition as that of the bulk anisotropy constant, i.e., $\tilde{k}_S\equiv 2K_S M_S^2/J_{BB}M_B^2=\gamma k_S$. Moreover, the definition of k_S can also depend on specific requirements arising when one needs to compare theoretical results to a concrete set of experimental data. We stress, however, that all the conclusions obtained in the present work remain the same regardless of the choice of the model parameters: $(\gamma,\tilde{k}_S,k_B)$ or (γ,k_S,k_B). In order to switch from the parameters (γ,k_S,k_B) used here to model parameters $(\gamma,\tilde{k}_S,k_B)$ one should substitute k_S with $\tilde{k}_S/\gamma$ in each formula. The diagrams of magnetic states in the coordinates $(\gamma,\tilde{k}_S,k_B)$ and (γ,k_S,k_B) look similar. The differences between these diagrams are only those naturally following from the redefinition of the surface anisotropy constant $k_S\to\tilde{k}_S/\gamma$. Thus, in the coordinates (γ,k_S,k_B) the in-plane state exists only for $k_S>-1$, whereas in the new coordinates $(\gamma,\tilde{k}_S,k_B)$ it exists only for $\tilde{k}_S>-\gamma$. Similarly, in the coordinates (γ,k_S,k_B) the perpendicular state exists only for $k_S<+1$, whereas in new coordinates it exists only for $\tilde{k}_S<+\gamma$, etc.

For $N=2$, the criterion of the perpendicular state in new coordinates can be written as $k_B<\gamma\tilde{k}_S/(\tilde{k}_S-\gamma)$. In the limiting case $\gamma\to+\infty$, it transforms into $k_B<-\tilde{k}_S$. For $N=2$, the criterion of the in-plane state in the new coordinates can be written as $k_B>-\gamma\tilde{k}_S/(\tilde{k}_S+\gamma)$. In the limiting case $\gamma\to+\infty$, it transforms into $k_B>-\tilde{k}_S$. Therefore, in the case of $N=2$ and of an infinite exchange interaction between two atomic layers, $\gamma\to+\infty$, there is a direct competition between surface and bulk anisotropy energies discussed above. In fact, for $N=2$ in the limiting case of $\gamma\to+\infty$, when two atomic layers appear to be strongly coupled, we come back to model (1), which does not allow for the canted noncollinear state.

For $N=3$, the stability criterion of the perpendicular state [Eq. (A11)] can be written in terms of $\tilde{k}_S$ and k_B as

$$\tilde{k}_S<\frac{\gamma k_B(k_B-2)}{k_B^2-(\gamma+2)k_B+\gamma}.$$

In the limiting case of $\gamma\to+\infty$, it transforms into

$$\tilde{k}_S<\frac{k_B(k_B-2)}{1-k_B}.$$

Adding k_B to both sides of this inequality, we have

$$\tilde{k}_{Seff}\equiv\tilde{k}_S+k_B<\frac{k_B}{k_B-1}.$$

As expected, the last formula exactly coincides with the criterion of the stability of the perpendicular state for $N=2$ for $\gamma=1$ [Eq. (A7)], with the effective surface anisotropy constant $\tilde{k}_{Seff}\equiv\tilde{k}_S+k_B$. Obviously, in the limiting case $\gamma\to+\infty$, the three-layer film is equivalent to a bilayer with an effective surface layer consisting of strongly coupled surface and subsurface layers of the real three-layer film.

IV. EVOLUTION OF THE DIAGRAM OF MAGNETIC STATES WITH FILM THICKNESS

To study the evolution of borders between the different regions in the diagram with film thickness N, it is convenient to fix the parameter $\gamma>0$. Actually, we do not know the exact magnitude of this parameter for the Co/Au films; thus, for certainty, we put $\gamma=1$. The diagrams of magnetic states for $N=2$, 3, and 4 are presented in Fig. 4, together with the diagram for $N\to\infty$.

In Fig. 4, the region corresponding to the in-plane state is situated above the solid line of the color chosen for each N, and the existence region of the perpendicular state lies below the dashed line of the same color. The canted noncollinear state exists in the region between solid and dashed lines of the corresponding color. In the left part of the diagram, $k_S<0$, the in-plane-canted noncollinear border has the vertical asymptote $k_S=-1$. In the right part of this diagram, $k_S>0$, the perpendicular-canted noncollinear border has the vertical asymptote $k_S=+1$. The same asymptotes can be seen in the

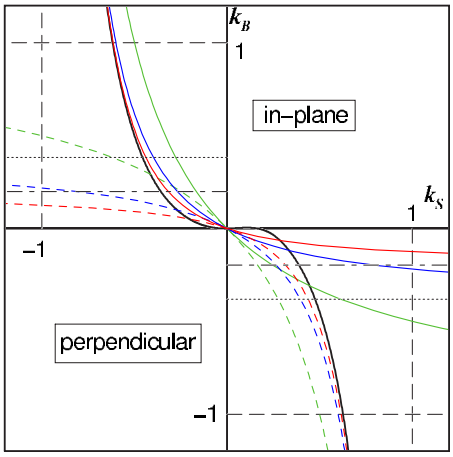

FIG. 4. (Color online) Diagrams of magnetic states in coordinates (k_S,k_B) for $N=2,3,4,\ldots,\infty$, $\gamma=1$. $N=2$, green; $N=3$, blue; $N=4$, red;..; $N=\infty$, black. For each fixed film thickness N, the region corresponding to the in-plane state is situated above the solid line, and the region corresponding to the perpendicular state is situated below the dashed line of the same color. The rest of the diagram corresponds to the canted noncollinear state. In the left part of the diagram, $k_S<0$, in the limiting case $N\to\infty$, the stability threshold of the perpendicular state of the semi-infinite film corresponds to the horizontal line $k_B=0$, and the stability threshold of the in-plane state of the semi-infinite film corresponds to the solid black line. Correspondingly, in the right side of the diagram, $k_S>0$, in the limiting case $N\to\infty$, the stability threshold of the in-plane state of the semi-infinite film corresponds to the horizontal line $k_B=0$, and the stability threshold of the perpendicular state of the semi-infinite film corresponds to the solid black line.

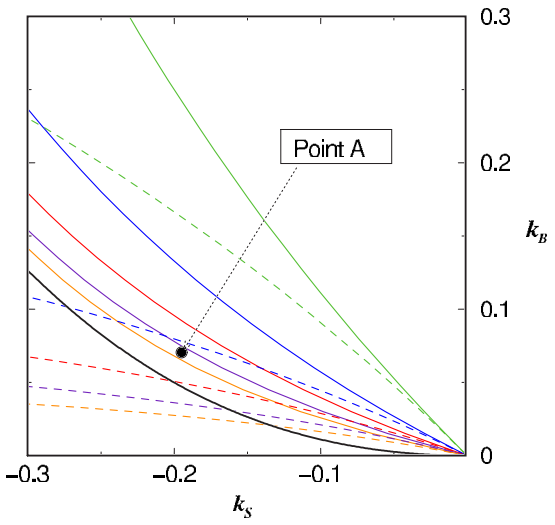

FIG. 5. (Color online) Diagram of magnetic states in coordinates (k_S,k_B). The film thickness $N=2,3,4,5,6,\ldots,\infty$. The parameter γ is chosen to be $\gamma=1$. $N=2$, green; $N=3$, blue; $N=4$, red; $N=5$, indigo; $N=6$, orange;..; $N=\infty$, black. For each N, the region corresponding to the canted noncollinear state is situated between the solid and dashed lines of the corresponding color. The stability region of the perpendicular state is situated below the dashed line, and the region corresponding to the in-plane state lies above the solid line.

diagram for a semi-infinite film (Fig. 4). These asymptotes appear as a result of the layer by layer approach used here. In contrast, in Refs. 31–34, where the continuum approach has been employed, the corresponding diagram has no vertical asymptotes because in this approach the anisotropy energy is assumed to be much smaller than the energy of the exchange interaction between atomic layers. Therefore, the continuum approach allows one to construct only a part of the diagram close to the coordinate origin. However, even in the vicinity of the coordinate origin, the usage of the continuum approach can lead to wrong results. Indeed, if the exchange interaction between the surface and subsurface atomic layers is much smaller than the exchange interaction between the bulk layers ($\gamma\ll 1$), then even a rather small (as compared to the exchange interaction in bulk) effective surface anisotropy energy ($\gamma<\tilde{k}_S\ll 1$) can cause the deviation of the surface magnetization from the in-plane orientation. In order to illustrate this, one should consider the diagram of the magnetic states in the $(\tilde{k}_S,k_B)$ coordinates. This diagram is similar to the (k_S,k_B) diagram presented in Fig. 4. The only difference is that in the $(\tilde{k}_S,k_B)$ diagram the vertical asymptotes are determined as $\tilde{k}_S=\pm\gamma$; i.e., in the case ($\gamma\ll 1$), they are very close to the coordinate origin. It means that in the case ($\gamma\ll 1$), a point $(\tilde{k}_S,k_B)$ even with a small effective surface anisotropy constant ($\gamma<\tilde{k}_S\ll 1$) can be situated in the region corresponding to the canted noncollinear state.

The left part of the diagram, $k_S<0$ (Fig. 4) demonstrates that as N increases, the dashed line representing the border between the perpendicular and canted noncollinear states shifts downward. In the limiting case $N\to\infty$, it coincides with the horizontal line $k_B=0$, which is the perpendicular-canted noncollinear border in the diagram for the semi-infinite case. With increasing N, the solid line, representing the border between the in-plane and canted noncollinear states, also moves downward in the left part of the diagram. In the limiting case $N\to\infty$, it coincides with the solid black line that is the border between the in-plane and canted noncollinear regions in the diagram for semi-infinite films. In the right part of the diagram, $k_S>0$, the in-plane-canted noncollinear border (solid line) moves upward as N becomes larger. In the limiting case $N\to\infty$, it coincides with the horizontal line $k_B=0$, which is the in-plane-canted noncollinear border in the diagram for a semi-infinite film. In the right part of the diagram, $k_S>0$, the dashed line that is the perpendicular-canted noncollinear border also moves upward as N becomes larger. In the limiting case $N\to\infty$, it coincides with the dashed black line that is the perpendicular-canted noncollinear border for the semi-infinite case.

Knowledge about the evolution of borders separating the stability regions for different magnetic states with film thickness allows one to qualitatively describe the SRT1 $m_\perp\to m_\angle$ and the SRT2 $m_\angle\to m_\parallel$ taking place in Co/Au films with increasing film thickness. Let us take a closer look at the left upper quadrant of the diagram, which is shown in Fig. 5 on a larger scale. In this part of the diagram, the surface anisotropy energy favors the perpendicular state,

whereas the bulk anisotropy energy favors the in-plane state. Let us specify a point A with coordinates (k_S^A, k_B^A), which are the reduced surface and bulk anisotropy constants of a bare Co/Au film. For the sake of simplicity, we assume that these coordinates do not depend on N; i.e., point A does not move in the diagram as the film thickness changes. The position of point A was chosen in such a way that for $N=2$ and $N=3$ the film is in the perpendicular state (point A is below the green and blue dashed lines in Fig. 5). For $N=4$, point A is above the dashed red line and below the solid red line; i.e., the film is in the canted noncollinear state. Therefore, changing N from 3 to 4, one should observe the SRT1 from the perpendicular state to the canted noncollinear state $m_\perp \rightarrow m_\angle$, that is, in accordance with experiments reporting that $N_{SRT1} \approx 3.5\ AL$.[13] For $N=5$, the film is still in the canted noncollinear state because point A is above the dashed indigo line and below the solid indigo line. Further increase in the film thickness up to $N=6$ leads to the SRT2 from the canted noncollinear state to the in-plane state, $m_\angle \rightarrow m_\parallel$, as for $N=6$ point A is already situated above the solid orange line. Again, this agrees with experiment, which gives $N_{SRT2} \approx 5.5\ AL$.[13] Note that it is not just one point in the diagram but rather a region, which corresponds to experimental results: $N_{SRT1} \approx 3.5\ AL$ and $N_{SRT2} \approx 5.5\ AL$. In this region $k_S \in (-0.24; -0.1)$, $k_B \in (0.03; 0.09)$, and the ratio $|k_S/k_B|$ is equal to 2.7 ± 0.3.

V. SMALL REDUCED BULK ANISOTROPY CONSTANT k_B AS A LIMITING CASE

In the case of an arbitrary reduced bulk anisotropy constant k_B, the analytic expressions for the stability criteria of the perpendicular state [Eqs. (A22) and (A26)] and the in-plane state [Eqs. (B3) and (B5)] are too bulky. However, there exist many magnetic layered systems with rather small k_B, such as Fe and Ni. Therefore, we find it useful to explicitly consider the limiting case of small k_B as this would allow one to substantially simplify the procedure of the evaluation of anisotropy constants k_S and k_B from the comparison of theory and experiment in the case $|k_B| \ll 1$.

The comparison of the thermodynamic potentials of the perpendicular and in-plane states, Eqs. (8) and (9), gives

$$\varphi_\perp - \varphi_\parallel = \frac{1}{2}\sum_{n=1}^{N} k_n = \frac{1}{2}[\gamma k_S + (N-1)k_B] \equiv \frac{(N-1)}{2}\left(k_B + \frac{\gamma k_S}{N-1}\right). \quad (12)$$

It follows from Eq. (12) that the parameter $(N-1)$ plays a role of the film thickness. In the (k_S, k_B) diagram of the thermodynamic potentials for the perpendicular and in-plane states are equal to each other on the straight line defined as

$$k_S = -\frac{N-1}{\gamma}k_B. \quad (13)$$

In accordance with Eq. (12), the in-plane state is favorable for $N > (k_B - \gamma k_S)/k_B$ and the perpendicular state is favorable for $N < (k_B - \gamma k_S)/k_B$. So, it seems that the SRT $m_\perp \rightarrow m_\parallel$ is discontinuous. However, in the (k_S, k_B) diagram, both the perpendicular and in-plane states become unstable, not exactly at line $k_B = -\gamma k_S/N - 1$ but in some vicinity of this line.

Let us illustrate this statement in the limiting case ($|k_B| \ll 1$). In accordance with the solution of model (3) presented in Appendixes A and B, the perpendicular state is stable when $k_S \leqslant k_{SC}^{\perp}(k_B, N, \gamma)$ [Eqs. (A22) and (A26)], and the in-plane state is stable if $k_S \geqslant k_{SC}^{\parallel}(k_B, N, \gamma)$ [Eqs. (B3) and (B5)]. The expansion of these expressions to the second order of k_B gives

$$m_\perp: k_S \leqslant k_{SC}^{\perp}(k_B, N, \gamma) = -\frac{(N-1)}{\gamma}k_B - \frac{(N-1)[2\gamma N^2 - (7\gamma - 6)N + 6(\gamma - 1)]}{6\gamma^2}k_B^2 + \cdots, \quad (14)$$

$$m_\parallel: k_S \geqslant k_{SC}^{\parallel}(k_B, N, \gamma) = -\frac{(N-1)}{\gamma}k_B + \frac{(N-1)[2\gamma N^2 - (7\gamma - 6)N + 6(\gamma - 1)]}{6\gamma^2}k_B^2 + \cdots. \quad (15)$$

It follows from Eqs. (14) and (15) that in the linear approximation with respect to k_B, the expressions for the stability threshold of the perpendicular and in-plane states coincide with each other. Consequently, the canted noncollinear state cannot be realized. Therefore, we conclude that the frequently used model (1) corresponds to the linear approximation with respect to k_B in the solution of model (3). However, in the quadratic approximation with respect to k_B, there is a finite nonzero range of k_S where the canted noncollinear state can take place.

$$m_\angle: k_{SC}^{\perp}(k_B, N, \gamma) < k_S < k_{SC}^{\parallel}(k_B, N, \gamma). \quad (16)$$

In the particular case of $\gamma = 1$, Eqs. (14) and (15) have the simplest form of

$$m_\perp: k_S \leqslant k_{SC}^{\perp}(k_B, N) \approx -(N-1)k_B - \frac{(N-1)N(2N-1)}{6}k_B^2, \quad (17)$$

$$m_\parallel: k_S \geqslant k_{SC}^{\parallel}(k_B, N) \approx -(N-1)k_B + \frac{(N-1)N(2N-1)}{6}k_B^2. \quad (18)$$

The (k_S, k_B) diagram for $N=3$ and $\gamma=1$ constructed in accordance with formulas (17) and (18) is presented in Fig. 6. Equations (17) and (18) can be used for an approximate determination of the reduced surface and bulk anisotropy constants, k_S and k_B, from the comparison of experiment and theory. Indeed, if experimental data supply us with N_{SRT1} corresponding to the onset of the SRT1 from the perpendicular to the canted noncollinear state $m_\perp \rightarrow m_\angle$ and with N_{SRT2} corresponding to the onset of SRT2 from the canted to the in-plane state $m_\angle \rightarrow m_\parallel (N_{SRT2} > N_{SRT1})$, then one should sub-

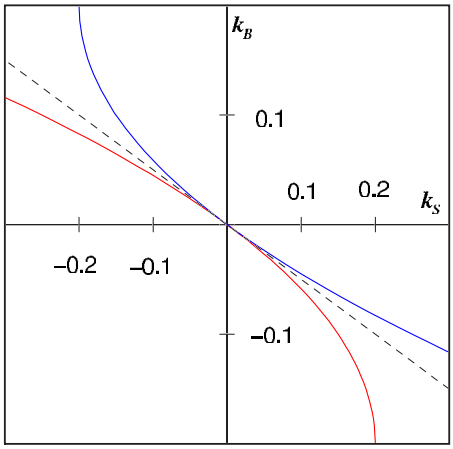

FIG. 6. (Color online) Diagram of magnetic states in coordinates (k_S, k_B) constructed in the approximation $|k_B| \ll 1$ in the particular case $\gamma=1$ in accordance with Eqs. (17) and (18). The region corresponding to the perpendicular state of a film is situated below the solid red line. The region corresponding to the in-plane state of a film is situated above the solid blue line. The region corresponding to the canted noncollinear state lies between the solid red and solid blue lines. The dashed straight line shows the equality of the thermodynamic potentials of the perpendicular and in-plane states [Eq. (13)].

stitute N with N_{SRT1} in Eq. (17) and with N_{SRT2} in Eq. (18) and, thus, get a simple set of two equations with the reduced anisotropy constants k_S and k_B.

VI. BILAYER FILM

In the present section, we consider the magnetic properties of a bilayer film with competing anisotropies at two sides of the bilayer and the ferromagnetic exchange interaction between atomic layers. Although, the problem of a bilayer has been considered theoretically many times before,[6,26] to the best of our knowledge it has never been solved properly. At the same time, bilayer is a system often found in both bulk and thin-film magnetism. Indeed, in a two layer ferromagnetic Co film deposited on Au substrata, the anisotropy energy of the Co-Au interface and that of the free surface are expected to be different. In a two layer Co film sandwiched between two nonmagnetic films such as Au/Co/W, the magnetic anisotropies of different interfaces should also be different. Two sublattices in a wide variety of ferrimagnetics can also exhibit different anisotropies. This, in turn, can lead to noncollinear magnetic structures often found, for instance, in compounds containing rare-earth metals. Integral to this is an artificially created magnetic multilayer structures with alternating magnetic and nonmagnetic layers such as Fe/V/Co/V/Fe/V/Co. In this multilayer, the Fe layers exhibit the in-plane anisotropy whereas Co layers exhibit the perpendicular anisotropy. The interplay between the anisotropy energies of neighbor Fe and Co layers and the ferromagnetic exchange interaction between them leads to a noncollinear magnetic structure. The magnetic properties of inner layers, far from the edges of the multilayer structure, have been described within a bilayer approach.[51] Finally, the consideration of the bilayer case helps to outline some issues such as the order of the SRT and the applicability of perturbation theory, which were not analyzed in the previous sections.

Here, we apply three different approaches in the investigation of a bilayer. The first approach is conducted entirely in the spirit of the present work; namely, it is devoted to the derivation of the stability criteria of the perpendicular and in-plane states. The corresponding formulas are presented in Appendix A [Eq. (A7)] and in Appendix B [Eq. (B6)], respectively. We have to note that the presence of the parameter γ in Eqs. (A7) and (B6) might mislead the reader. Recall that the parameter γ characterizes the nonuniformity of the exchange interaction in the surface region of a film, which in the case of bilayer does not make any sense. Because of that, in Eqs. (A7) and (B6) one should better put $\gamma=1$. This means that the anisotropy energies at both sides of the film are reduced by the exchange interaction between the two atomic layers in the bilayer. We keep an arbitrary $\gamma>0$ in Eqs. (A7) and (B6) just because we would like to stress that in the particular case of a bilayer, the general formulas for the stability criteria of the perpendicular and in-plane states of a film of thickness N [Eqs. (A22), (A26), (B3), and (B5)] give correct results [Eqs. (A7) and (B6)] for arbitrary γ. In addition, one should treat the diagram of the magnetic states of a bilayer in coordinates (γ, k_S, k_B) presented in Fig. 1 as a diagram in which all coordinates were obtained by dividing the corresponding energies with the exchange interaction between the layers in the bulk sample. Definitely, the bulk exchange interaction is absent in the bilayer, but it is present in bulk samples. Hence, one may use it for introducing the reduced model parameters. We hope this will not cause any misunderstanding in the treatment of the diagram for the bilayer shown in Fig. 1.

In this section, we mostly address the diagram of magnetic states of a bilayer presented in Fig. 4 (green dashed and solid lines). In this (k_S, k_B) diagram, the in-plane region is situated above the green solid line and the perpendicular region lies below the dashed green line. The canted noncollinear region is between the green dashed and solid lines. Here, we do not use the concept of the bulk anisotropy constant k_B because the very concept of a bulk layer is not applicable to the bilayer case. Hence, instead of parameters k_S and k_B used in the previous sections, we use the reduced anisotropy constants of each layer denoted here as $k_{S1} \equiv k_S$ and $k_{S2} \equiv k_B$. Then the stability criteria of the perpendicular [Eq. (A7)] and in-plane [Eq. (B6)] states of a bilayer can be written as

$$\begin{aligned} k_{S2} &< k_{S2\,\max}^{\perp} = 1, \\ k_{S1} &< k_{SC1}^{\perp}(N=2) = \frac{k_{S2}}{k_{S2}-1}, \\ k_{S2} &> k_{S2\,\min}^{\parallel} = -1, \end{aligned} \tag{19}$$

$$k_{S1} > k_{SC1}^{\parallel}(N=2) = -\frac{k_{S2}}{k_{S2}+1}. \tag{20}$$

In these formulas the parameter γ is set to 1. We have to note that similar analytic expressions for the stability criteria of the perpendicular and in-plane states were derived in Ref. 26. However, the authors of Ref. 26 presented only the second

line in Eqs. (19) and (20). No conditions for the parameter k_{S2} [first line in Eqs. (19) and (20)] were presented. We have to note that the function on the right side of the equation in the second line of Eqs. (19) and (20) is a hyperbola that consists two branches separated by two asymptotes, vertical and horizontal. Only one of these two branches represents the perpendicular-canted noncollinear and in-plane-canted noncollinear borders in the diagram, whereas the other branch is irrelevant. Therefore, it is unclear how the authors of Ref. 26 sorted out these lines in their work.

The derivation of the stability criteria of the perpendicular and in-plane states of a bilayer is certainly a useful result. However, it does not give any information about the order of the SRT1 $m_{\perp} \rightarrow m_{\angle}$ as well as about the order of the subsequent SRT2 $m_{\angle} \rightarrow m_{\parallel}$ observed in Co/Au films. Definitely, the variation of the essentially integer parameter N cannot shed light on the order of these SRTs. To approach this problem, we formulate it in the following way. Would the orientation angles θ_1 and θ_2 change continuously when a point crosses the border between the perpendicular and canted noncollinear states in the (k_S, k_B) diagram or would this change be discontinuous? The same question holds in the case of crossing the border between canted noncollinear and in-plane states. The approach described below will help one to answer these questions.

The second approach used in the present section is entirely based on the Landau theory of the second-order phase transitions. In the spirit of this theory, one should use the concept of the order parameter and expand the thermodynamic potential to the forth power of the order parameter,

$$\Phi = A\eta^2 + B\eta^4, \quad A = a(T - T_C), \quad a > 0. \tag{21}$$

It follows from Eq. (21) that coefficient A changes its sign with temperature at some point T_C called the Curie point. The phase transition with temperature at T_C is of the second order if coefficient B is positive. For $T > T_C$, the equilibrium magnitude of the order parameter is equal to zero. For $T < T_C$, the equilibrium value of the order parameter is defined as $\eta = \sqrt{a(T_C - T)/(2B)} \neq 0$. Since in the vicinity of the Curie point the order parameter η changes continuously with temperature, the second-order phase transition is often called a continuous phase transition.

Hence, following the Landau theory, one should choose an order parameter, expand the thermodynamic potential to the fourth order of the order parameter, and analyze the sign of coefficients A and B. In terms of the model parameters introduced above, the expression for the thermodynamic potential of a bilayer can be written as

$$\varphi = -\cos(\theta_1 - \theta_2) + \frac{k_{S1}}{2}\sin^2\theta_1 + \frac{k_{S2}}{2}\sin^2\theta_2. \tag{22}$$

The minimization of the thermodynamic potential [Eq. (22)], with respect to each of the orientation angles θ_1 and θ_2, gives rise to the set of equations with respect to θ_1 and θ_2,

$$\frac{\partial\varphi}{\partial\theta_1} = \sin(\theta_1 - \theta_2) + k_{S1}\sin\theta_1\cos\theta_1 = 0,$$

$$\frac{\partial\varphi}{\partial\theta_2} = -\sin(\theta_1 - \theta_2) + k_{S2}\sin\theta_2\cos\theta_2 = 0. \tag{23}$$

We first investigate the solution of Eq. (23) in the vicinity of the in-plane-canted noncollinear border where the orientation angles θ_1 and θ_2 are small, $\theta_{1,2} \ll 1$. Bearing this in mind, one can express the orientation angle θ_2 via the orientation angle θ_1, and the corresponding expression can be expanded to the third power of θ_1

$$\theta_2 = \frac{1}{2}\arcsin\left(\frac{k_{S1}}{k_{S2}}\sin 2\theta_1\right) \cong -\frac{k_{S1}}{k_{S2}}\theta_1 + \frac{2}{3}\frac{k_{S1}}{k_{S2}}\left[1 - \left(\frac{k_{S1}}{k_{S2}}\right)^2\right]\theta_1^3. \tag{24}$$

Then, one should expand the thermodynamic potential [Eq. (21)] to the fourth power of each of the orientation angles θ_1, θ_2, and substitute θ_2, with the expression given by Eq. (24). After some algebra, the final expression for the part of the thermodynamic potential dependent on angle θ_1 can be written as

$$\Delta\varphi = \frac{1}{2}\left[k_{S1} - \left(\frac{-k_{S2}}{k_{S2}+1}\right)\right]\theta_1^2 + \frac{k_{S2}^2(k_{S2}+2)^2}{8(k_{S2}+1)^4}\theta_1^4. \tag{25}$$

It follows from Eq. (25) that the first orientation angle θ_1 plays the role of an order parameter, and the expression for the thermodynamic potential can be written in a form characteristic of the Landau theory of the second-order phase transitions. The comparison of Eqs. (25) and (21) shows that the parameter k_{S1} plays the role of temperature. The expression corresponding to the Curie temperature in Eq. (25) is determined by the expression $k_{SC1} = -k_{S2}/(k_{S2}+1)$, which exactly coincides with the analytic expression of the stability criterion of the in-plane state [Eq. (20)]. The comparison of Eqs. (21) and (25) also shows that coefficient B, the second term in Eq. (25), is positive. Therefore, we have to conclude that in the diagram of the magnetic states of a bilayer, the crossing of the in-plane-canted noncollinear border corresponds to the continuous second-order phase transition (solid green line in Fig. 4).

To analyze the order of phase transition taking place at the border between the perpendicular and canted noncollinear regions, one should better introduce new orientation angles $\alpha_i = \pi/2 - \theta_i$ and use the first orientation angle α_1 as an order parameter. In the vicinity of this border, the orientation angles α_1 and α_2 are small, $\alpha_{1,2} \ll 1$. Bearing this in mind, one can perform a similar procedure to that used above and again derive the expression for the part of the thermodynamic potential dependent on angle α_1,

$$\Delta\varphi = -\frac{1}{2}\left(k_{S1} - \frac{k_{S2}}{k_{S2}-1}\right)\alpha_1^2 + \frac{k_{S2}^2(k_{S2}-2)^2}{8(k_{S2}-1)^4}\alpha_1^4. \tag{26}$$

The analyses of Eq. (26) bring us to the conclusion that in the diagram of the magnetic states of a bilayer, crossing the perpendicular-canted noncollinear border corresponds to the second-order phase transition (green dashed line in Fig. 4). In the present work, we do not perform the analysis of the order of phase transitions for a film of arbitrary N. So far, we

analyzed the order of the SRT $m_{\parallel} \rightarrow m_{\angle}$ with temperature only for a semi-infinite sample described by model (3).[50] Nevertheless, we are convinced that in the diagram of the magnetic states of thin films, all the borders correspond to the second-order phase transitions. Indeed, taking into account the anisotropy constants of the lowest order and finite exchange interaction always results in a continuous phase transition. To describe the discontinuous phase transition, one should take into account either the higher order anisotropies or the dependence of the exchange integral on distance, or the biquadratic exchange interaction. The model considered in this work, Eq. (2) or (3), does not contain such terms.

Actually in our treatment of the SRT $m_{\perp} \rightarrow m_{\parallel}$ with film thickness observed in Co/Au films, we do not move any point in the diagram of magnetic states. We assume that point $A(k_S, k_B)$ corresponding to the Co/Au film is motionless (Sec. IV). The SRT is described using the fact that both the perpendicular-canted noncollinear border and the in-plane-canted noncollinear border move with film thickness, thus changing their positions with respect to the point $A(k_S, k_B)$. Since the crossing of each of these borders corresponds to the continuous second-order phase transition, we consider the spin reorientation observed in Co/Au films as a two-step SRT consisting of two subsequent *continuous second-order SRTs*: SRT1 $m_{\perp} \rightarrow m_{\angle}$ and SRT2 $m_{\angle} \rightarrow m_{\parallel}$.

The third approach used in this section for the investigation of the magnetic properties of a bilayer is based on the analytical solution of the system of equations for the orientation angles θ_1 and θ_2 [Eq. (23)]. We have to note that this system of equations has many solutions both trivial (such as $\theta_1=\theta_2=0$, and $\theta_1=\theta_2=\pi/2$) and nontrivial, corresponding to a canted noncollinear state. Here, we search only for nontrivial solutions. The number of nontrivial solutions is also large. However, they are symmetrical; i.e., if θ_1 and θ_2 satisfy the system of equations [Eq. (23)], then $\pi-\theta_1$ and $\pi-\theta_2$ also satisfy this system of equations as well as $-\theta_1$ and $-\theta_2$, etc. Here, we only search for the nontrivial solution in the interval $(0, \pi/2)$.

It follows from Eq. (23) that the following equality is valid:

$$k_{S1} \sin\theta_1 \cos\theta_1 + k_{S2} \sin\theta_2 \cos\theta_2 = 0. \tag{27}$$

Since $\theta_i \in (0, \pi/2)$, the nontrivial solution is possible only if the anisotropy constants k_{S1} and k_{S2} have different signs, i.e., only in the case of competing anisotropies at two sides of the bilayer. Dividing Eq. (27) by $\cos^2\theta_1$ and by $\cos^2\theta_2$ allows one to rewrite Eq. (27) in terms only of tangents of the corresponding orientation angles

$$k_{S1} tg\theta_1 (tg^2\theta_2 + 1) + k_{S2} tg\theta_2 (tg^2\theta_1 + 1) = 0. \tag{28}$$

Dividing each equation in Eq. (23) by $\cos\theta_1 \cos\theta_2$ allows one to rewrite Eq. (23) in the form

$$tg\theta_1 - tg\theta_2 = -k_{S1} tg\theta_1 \frac{\cos\theta_1}{\cos\theta_2},$$

$$tg\theta_1 - tg\theta_2 = k_{S2} tg\theta_2 \frac{\cos\theta_2}{\cos\theta_1}. \tag{29}$$

Having multiplied these equations, one obtains the following quadratic form:

$$tg^2\theta_2 - (2 - k_{S1}k_{S2}) tg\theta_1 tg\theta_2 + tg^2\theta_1 = 0. \tag{30}$$

The solution of Eq. (30) with respect to $tg\theta_2$ gives a simple relation between $tg\theta_1$ and $tg\theta_2$: $tg\theta_2 = \lambda_{\pm} tg\theta_1$, where $\lambda_{\pm}$ are determined as

$$\lambda_{\pm} = \frac{1}{2}[2 - k_{S1}k_{S2} \pm \sqrt{k_{S1}k_{S2}(k_{S1}k_{S2} - 4)}]. \tag{31}$$

Finally, the substitution of $tg\theta_2$ by the expression $tg\theta_2 = \lambda_{\pm} tg\theta_1$ in Eq. (28) allows one to express $tg\theta_1$ and $tg\theta_2$ using the model parameters

$$tg^2\theta_1 = -\frac{k_{S1} + \lambda_{\pm}k_{S2}}{\lambda_{\pm}^2 k_{S1} + \lambda_{\pm}k_{S2}},$$

$$tg^2\theta_2 = -\frac{\lambda_{\pm}(k_{S1} + \lambda_{\pm}k_{S2})}{\lambda_{\pm}k_{S1} + k_{S2}}. \tag{32}$$

It turns out that it is more convenient to deal with cosines rather than with tangents. The corresponding formulas for cosines follow from Eq. (32). Simple analyses show that in the left part of the (k_{S1}, k_{S2}) diagram, $k_{S1}<0$, the expressions for $\cos^2\theta_1$ and $\cos^2\theta_2$ are determined by the following formulas:

$$\cos^2\theta_1 = \frac{\lambda_-(\lambda_- k_{S1} + k_{S2})}{k_{S1}(\lambda_-^2 - 1)},$$

$$\cos^2\theta_2 = -\frac{(\lambda_- k_{S1} + k_{S2})}{k_{S2}(\lambda_-^2 - 1)}, \qquad k_{S1} < 0. \tag{33}$$

In the right part of the (k_{S1}, k_{S2}) diagram, $k_{S1}>0$, the expressions for $\cos^2\theta_1$ and $\cos^2\theta_2$ are determined by the following formulas:

$$\cos^2\theta_1 = \frac{\lambda_+(\lambda_+ k_{S1} + k_{S2})}{k_{S1}(\lambda_+^2 - 1)},$$

$$\cos^2\theta_2 = -\frac{(\lambda_+ k_{S1} + k_{S2})}{k_{S2}(\lambda_+^2 - 1)}, \qquad k_{S1} > 0. \tag{34}$$

Here, we restrict our investigation by the consideration only of Eq. (34) that corresponds to the left part of the (k_{S1}, k_{S2}) diagram, $k_{S1}<0$. The analysis of Eq. (35) that corresponds to the right part of the (k_{S1}, k_{S2}) diagram, $k_{S1}>0$, is quite similar.

In Eq. (34), the requirement $\cos\theta_i=0$, $i=1,2$ leads to the condition $\lambda_- k_{S1} + k_{S2} = 0$ for both θ_1 and θ_2. In the (k_{S1}, k_{S2}) diagram, $k_{S1}<0$, this condition is satisfied at the perpendicular-canted noncollinear border (green dashed line in Fig. 4) determined by the equation $k_{S1} = k_{S2}/(k_{S2}-1)$. This means that at this border, each of orientation angles θ_1 and θ_2 is equal to $\pi/2$. In Eq. (34), the condition $\cos\theta_i=1$, $i=1,2$ leads to the equality $k_{S1} + \lambda_- k_{S2} = 0$ for both θ_1 and θ_2. In the (k_{S1}, k_{S2}) diagram, $k_{S1}<0$, this equality is satisfied at the canted noncollinear-in-plane border (green solid line in Fig.

4) determined by the equation $k_{S1}=-k_{S2}/(k_{S2}+1)$. This means that at this border, both θ_1 and θ_2 are equal to zero. Between the perpendicular-canted noncollinear and the canted noncollinear-in-plane borders, both $\cos^2\theta_1$ and $\cos^2\theta_2$ satisfy the condition $0<\cos^2\theta_{1,2}<1$; i.e., between these borders (green dashed and green solid lines in Fig. 4), the canted noncollinear state is realized. In the region corresponding to the perpendicular state of a bilayer $k_{S1}<k_{S2}/(k_{S2}-1)$, below the green dashed line in Fig. 4, $\cos^2\theta_{1,2}<0$; i.e., the canted noncollinear state cannot be realized; thus, the perpendicular state takes place. In the region corresponding to the in-plane state, $k_{S1}>-k_{S2}/(k_{S2}+1)$, above the green solid line in Fig. 4, $\cos^2\theta_{1,2}>1$, i.e., again the canted noncollinear state cannot be realized and, thus, the in-plane state takes place. Therefore, on the movement of an imaginary point in the (k_{S1},k_{S2}) diagram, $k_{S1}<0$, the crossing of the perpendicular-canted noncollinear border leads to a continuous decrease in orientation angles $\theta_{1,2}$ from $\pi/2$ in the perpendicular region to smaller magnitudes in the canted noncollinear region. Further movement of the point toward the canted noncollinear-in-plane border leads to a further decrease in orientation angles $\theta_{1,2}$ down to zero at the noncollinear-in-plane border. In the in-plane region, both orientation angles are zero, $\theta_{1,2}\equiv 0$.

The analytic results for the orientation angles of a bilayer could be useful for the verification of the validity of the perturbation theory often used for solving the bilayer problem.[6,36] In these works, another definition of the orientation angles is used: $\alpha_i=\pi/2-\theta_i$. Then the average orientation angle is introduced $\bar{\alpha}=(\alpha_1+\alpha_2)/2$, and the so-called small parameter of the perturbation theory is defined as $\varepsilon_i \equiv \alpha_i-\bar{\alpha}$, $\varepsilon_1=(\alpha_1-\alpha_2)/2$, and $\varepsilon_2=(\alpha_2-\alpha_1)/2$. The perturbation theory is believed to be applicable if the condition

$$\left|\frac{\varepsilon_i}{\bar{\alpha}}\right| \equiv \left|\frac{\alpha_1-\alpha_2}{\alpha_1+\alpha_2}\right| \ll 1 \tag{35}$$

is satisfied. To investigate this problem, we have to note that following Eq. (33), the following relation is valid:

$$\cos^2\theta_1 = K\cos^2\theta_2, \quad K \equiv -\lambda_- \frac{k_{S2}}{k_{S1}}. \tag{36}$$

Therefore, in the case $K=1$, the orientation angles are equal to each other and, thus, the perturbation theory is valid. The larger the deviation of the coefficient K from 1 is, the larger the deviation ε_i of the orientation angles from the average value $\bar{\alpha}$ becomes and the less applicable the perturbation theory is. A simple analysis shows that in the vicinity of the in-plane-canted noncollinear border, coefficient K is equal to 1. Hence, in the vicinity of this border, the perturbation theory works well. In the vicinity of the perpendicular-canted noncollinear border, coefficient K is determined by the formula $K=(1-k_{S2})^2$. Taking this into account, relation (36) can be rewritten in the vicinity of this border in terms of new orientation angles in the following way:

$$\sin\alpha_1 = (1-k_{S2})\sin\alpha_2. \tag{37}$$

Since in the vicinity of the perpendicular-canted noncollinear border the orientation angles α_1 and α_2 are small, one may substitute Eq. (37) by $\alpha_1 \cong (1-k_{S2})\alpha_2$. Then, Eq. (35) can be written as

$$\left|\frac{\varepsilon_i}{\bar{\alpha}}\right| \equiv \left|\frac{\alpha_1-\alpha_2}{\alpha_1+\alpha_2}\right| = \frac{k_{S2}}{2-k_{S2}}, \quad k_{S2}\in(0,1). \tag{38}$$

It follows from Eq. (38) that the smaller the magnitude of parameter k_{S2} is, the more valid the perturbation theory is. Therefore, the perturbation theory should work well in the vicinity of the coordinate origin.

VII. CONCLUSIONS

The magnetic properties of ferromagnetic films with competing surface and bulk anisotropies and nonuniform exchange interaction between atomic layers have been investigated. The analytic expressions for the stability criteria of the perpendicular and in-plane states of a film of an arbitrary thickness have been derived in the framework of the layer by layer approach. We find that in a film characterized by an arbitrary layer-dependent ferromagnetic exchange interaction between atomic layers and by the layer-dependent anisotropy constants, a canted noncollinear state is favorable if neither the perpendicular nor in-plane state is stable. The diagram of the magnetic states of such films is presented, and the behavior of the magnetic state of the film depending on its thickness is analyzed. The applicability of the developed theory to realistic magnetic systems is demonstrated for the case of the two-step spin-reorientation transition observed in bare Co/Au films. The analytic solution of the bilayer problem is presented.

At present, a direct comparison of our theoretical results with data obtained in experiments for systems, such as Fe/Cu and Ni/Cu, is hardly possible. First, the domain wall width in Fe and Ni is too large compared to the film thickness. Because of that, the canted noncollinear state cannot develop well in these films; i.e., the deviation of the magnetization vector of neighbor atomic layers from each other is too small. Therefore, we stress once again that for the most part in the present work, we focus on the consideration of the canted noncollinear state. Second, the SRT in Fe/Cu goes via the stripe domain structure, which is a nonuniform state in the film plane. However, in the present work, we only consider states that are uniform in the film plane.

Formally, the reversed SRT in Ni/Cu films with film thickness from the in-plane to the perpendicular state could be described within the proposed model. However, we believe that such a description would be too rough as the model used in the present work is not really adequate for the Ni/Cu system. Thin Ni films on Cu(001) and Cu(111) exhibit a tetragonal lattice distortion in the pseudomorphic growth range near the interface. This distorted fcc symmetry exhibits a strong second-order magnetocrystalline anisotropy of the corresponding film layers. With increasing thickness, the strain in the Ni layers with a sufficient distance from the Ni-Cu interface is released and the corresponding strain anisotropy disappears for these layers. The detailed description of this physical picture is presented in the review of Ref. 6 (first paragraph in the left column on p. 152). Bearing this in

mind, one has to conclude that in contrast to the Co/Au system, the interface anisotropy energy in a Ni/Cu film is distributed among many Ni atomic layers in the interface region. Because of that, the ascription of the interface anisotropy constant to only one Ni atomic layer nearest to the Ni-Cu interface seems to us to be a too rough approach. Also, one has to conclude that the interface anisotropy energy depends on Ni film thickness. It means that the reversed SRT in the Ni/Cu film should be treated as a movement of the point corresponding to this system in the (k_S, k_B) diagram with film thickness rather than the movement of the borders between regions with film thickness. In other words, one may not treat the point corresponding to the Ni/Cu system as motionless. However, in the present paper, we do not analyze the dependence of anisotropy constants in the Ni/Cu system on film thickness. Because of the reasons presented above, we do not perform a detailed comparison of theoretical results obtained in the present work with experimental results related to Fe/Cu and Ni/Cu systems.

We believe that besides bare Co/Au films, the most suitable experimental systems to be compared with our theory could be magnetic sandwiches such as Au/Co/Au, Au/Co/W, etc. First, these sandwiches demonstrate similar SRTs with film thickness. The only difference is that compared to the case of bare Co/Au films, the onset of the SRT is shifted to larger film thicknesses. The nonmonotone dependence of coercive force on film thickness was discovered in these sandwiches.[18] This phenomenon is very interesting. To our opinion, it is caused by the difference between anisotropy constants at two interfaces. However, to describe the SRT and the nonmonotone dependence of coercive force on film thickness in these sandwiches, one should take into account the difference of the anisotropy constants at both sides of the film and the bulk anisotropy constant. This, in turn, means that the model used in the present work should be generalized for the case of arbitrary anisotropy constants at both sides of the film. Currently, this problem is under our consideration. We plan to present theoretical results related to the description of these phenomena in sandwiches Au/Co/Au and Au/Co/W in the nearest future.

ACKNOWLEDGMENTS

We are thankful to V. D. Borman and V. N. Tronin for a critical reading of the manuscript and for fruitful discussions.

APPENDIX A: STABILITY CRITERION OF THE PERPENDICULAR STATE OF A FILM OF FINITE THICKNESS

The investigation of the stability of the perpendicular state implies the analysis of an increment in the thermodynamic potential [Eq. (3)] caused by a small deviation of the magnetization vector of each atomic layer from the perpendicular orientation. If this increment is positive, the perpendicular state is stable; when it becomes negative, the perpendicular state is no longer stable. Bearing this in mind, we introduce new orientation angles $\alpha_n = \theta_n - \pi/2$ and expand the thermodynamic potential [Eq. (3)] to the second order of every α_n. The linear terms of the first order of α_n are absent in such an expansion because the necessary condition for the thermodynamic potential to be minimal is the zero value of its first derivative with respect to every α_n. Then, the increment in the thermodynamic potential $\Delta\varphi$ can be written in the following form:

$$\Delta\varphi = \vec{\alpha}^T \hat{A} \vec{\alpha}, \tag{A1}$$

where $\vec{\alpha} = (\alpha_1, \alpha_2, \alpha_3, \ldots, \alpha_N)$. Operator $\hat{A}$ in Eq. (A1) corresponds to a square $(N \times N)$ three-diagonal symmetrical matrix with real matrix elements,

$$A_{N\times N} = \begin{Vmatrix} \frac{\gamma(1-k_S)}{2} & -\frac{\gamma}{2} & 0 & 0 & \ldots & 0 & 0 & 0 \\ -\frac{\gamma}{2} & \frac{-k_B+\gamma+1}{2} & -\frac{1}{2} & 0 & \ldots & 0 & 0 & 0 \\ 0 & -\frac{1}{2} & -\frac{k_B}{2}+1 & -\frac{1}{2} & \ldots & 0 & 0 & 0 \\ 0 & 0 & -\frac{1}{2} & -\frac{k_B}{2}+1 & \ldots & \ldots & \ldots & \ldots \\ \ldots & \ldots & \ldots & \ldots & \ldots & \ldots & \ldots & \ldots \\ 0 & 0 & 0 & 0 & \ldots & -\frac{k_B}{2}+1 & -\frac{1}{2} & 0 \\ 0 & 0 & 0 & 0 & \ldots & -\frac{1}{2} & -\frac{k_B}{2}+1 & -\frac{1}{2} \\ 0 & 0 & 0 & 0 & \ldots & 0 & -\frac{1}{2} & -\frac{k_B}{2}+\frac{1}{2} \end{Vmatrix}. \tag{A2}$$

Then, one should find the necessary and sufficient conditions for the quadratic form [Eq. (A1)] to be positive. The positivity of the quadratic form resulting from the expansion of a function into a series in the vicinity of some point means that at this point the function is minimal.

The necessary and sufficient conditions for the quadratic form [Eq. (A1)] to be positive could be obtained using the Silvestre criterion known from the linear algebra. In accordance with this criterion, the necessary and sufficient condition for the quadratic form [Eq. (A1)] to be positive is reduced to the requirement that each corner minor of matrix A in Eq. (A2) must be positive,

$$d_1A \equiv |A_{11}| > 0, \quad d_2A \equiv \begin{vmatrix} A_{11} & A_{12} \\ A_{21} & A_{22} \end{vmatrix} > 0,$$

$$d_3A \equiv \begin{vmatrix} A_{11} & A_{12} & A_{13} \\ A_{21} & A_{22} & A_{23} \\ A_{31} & A_{32} & A_{33} \end{vmatrix} > 0, \quad \cdots . \tag{A3}$$

The deviation of the diagonal elements in the upper left corner of matrix (A2) from $-k_B/2+1$ as well as the deviation of the off-diagonal matrix elements from $-1/2$ is caused by the presence of a perturbation at the Co-Au interface. The origin of this perturbation is the following. First, the exchange interaction between the interface Co-Au layer and the neighbor Co layer differs from the exchange interaction between all the other Co layers. Second, there is no exchange interaction between the Co-Au layer and the neighbor Au layer. Here, we do not take into account the effect of magnetizing Au layers close to the Co-Au interface. Third, the interface anisotropy constant differs from the bulk anisotropy constant of Co. The difference between the diagonal element in the down right corner of matrix (A2) and all the other diagonal elements, $-k_B/2+1$, is caused by the presence of a perturbation at the surface of the Co film that is not covered by Au. It originates from the absence of the exchange interaction between the surface Co layer and vacuum above the free surface.

Introducing the notations $\varepsilon \equiv -k_B/2+1$ and $\delta \equiv (-k_S+k_B)/2$, it is possible to characterize all the matrix elements in Eq. (A2) affected by surface and interface perturbations at both sides of the Co film as

$$A_{11} = \varepsilon - \frac{1}{2} + \delta + \frac{k_S}{2}(\gamma - 1) + \frac{(\gamma - 1)}{2}, \quad A_{22} = \varepsilon + \frac{(\gamma - 1)}{2},$$

$$A_{12} = A_{21} = -\frac{1}{2} + \frac{(\gamma - 1)}{2}, \quad A_{NN} = \varepsilon - \frac{1}{2}. \tag{A4}$$

It follows from Eq. (A4) that all surface perturbations mentioned above are formally determined by the presence of the term $-1/2$ in A_{11} and A_{NN} and the term δ in A_{11}, as well as by the terms proportional to $(\gamma-1)$ in each matrix element in Eq. (A4).

Before the evaluation of the general expression for the stability criterion of the perpendicular state of a film of arbitrary N, it is worth formulating this criterion for several particular cases: $N=1$, 2, 3, and 4. One should do this as the corresponding matrices A for $N=1$, 2, and 3 do not coincide with the general form of matrix (A2), and they start to coincide with it only for $N \geqslant 4$. Moreover, the validity of the general formula for the stability criterion must be verified by comparing the general result with those obtained in several particular cases. Finally, the consideration of those particular cases allows one to reveal some trends in the evolution of the criterion with film thickness N, which we shall later use in the derivation of the general formula.

$N=1$. We assume that the magnetic Co film does not interact with the neighbor Au layers as we do not account for the effect of magnetizing neighbor Au layers by the Co monolayer. Most likely, this approximation is wrong for a Co monolayer deposited on Pd substrata because, in contrast to Au, Pd exhibits substantial polarizability. By this reason, for the Co/Au film all the exchange interactions in model (2) are equal to zero and the transition from Eq. (2) to the reduced thermodynamic potential [Eq. (3)] is not correct. In this case, one should analyze model (2) that for $N=1$ contains only one term $K_S M_S^2 \sin^2 \theta_1$. Hence, if $K_S<0$, then the perpendicular state $\theta_1=\pi/2$ is favorable; if $K_S>0$, then the in-plane state $\theta_1=0$ is favorable.

$N=2$. Matrix $A_{2\times 2}$ has the following form:

$$A_{2\times 2} = \begin{Vmatrix} \dfrac{\gamma(1-k_S)}{2} & -\dfrac{\gamma}{2} \\ -\dfrac{\gamma}{2} & \dfrac{-k_B+\gamma}{2} \end{Vmatrix}. \tag{A5}$$

From the requirement of the positivity of the first minor d_1A of matrix (A5), we get the first condition for the surface anisotropy constant k_S,

$$d_1A = \frac{\gamma(1-k_S)}{2} > 0 \Rightarrow k_S < 1, \tag{A6}$$

which will be repeated in the analyses of the sign of d_1A for arbitrary N. Because of that, further on we shall not mention condition (A6) and believe it is always satisfied. The requirement $d_2A>0$ can be written as $k_S(k_B-\gamma)>k_B$. If $k_B>\gamma$, then the parameter k_S must satisfy the condition $k_S>k_B/(k_B-\gamma)$. However, this condition is in contradiction with the condition $k_S<1$ [Eq. (A6)]. Hence, k_B must satisfy the opposite condition $k_B<\gamma$. This result is remarkable since in the considered case, the parameter $\gamma>0$ can formally be arbitrarily large and, thus, the perpendicular state can be realized for an arbitraril large k_B, satisfying the condition $k_B<\gamma$. In contrast to this, it will be shown below that for $N>2$, the maximal magnitude of k_B corresponding to the perpendicular state is always bounded from above. Finally, the stability criterion of the perpendicular state for $N=2$ is determined by the following formulas:

$$k_B < k_{B\,\max}^{\perp}(2) = \gamma,$$

$$k_S < k_{SC}^{\perp}(2) = \frac{k_B}{k_B - \gamma}. \tag{A7}$$

$N=3$. Matrix $A_{3\times3}$ has the following form:

$$A_{3\times3}=\begin{Vmatrix} \frac{\gamma(1-k_S)}{2} & -\frac{\gamma}{2} & 0 \\ -\frac{\gamma}{2} & \frac{-k_B+\gamma+1}{2} & -\frac{1}{2} \\ 0 & -\frac{1}{2} & -\frac{k_B}{2}+\frac{1}{2} \end{Vmatrix}. \quad \text{(A8)}$$

The requirement $d_1A>0$ leads to the condition $k_S<1$ [Eq. (A6)]. The requirement $d_2A>0$ can be written as $k_S[k_B-(\gamma+1)]>k_B-1$. If $k_B>(\gamma+1)$, then k_S must satisfy the condition $k_S>(k_B-1)/[k_B-(\gamma+1)]$. However, this condition is in contradiction with the condition $k_S<1$ [Eq. (A6)]. Therefore, k_B must satisfy the opposite condition $k_B<(\gamma+1)$; thus, k_S must satisfy the condition $k_S<(k_B-1)/[k_B-(\gamma+1)]$. We have to note that the latter condition for k_S is more restrictive than condition (A6). This implies the following: The requirement of the positivity of each next minor results in more restrictive conditions for k_S and k_B than the condition that follows from the requirement of the positivity of the previous minor. The requirement $d_3A>0$ for matrix (A8) can be written as

$$k_S[k_B^2-k_B(\gamma+2)+\gamma]<k_B(k_B-2). \quad \text{(A9)}$$

One can show that the possible values of the parameter $(\gamma+1)$ lie within the interval limited by the solutions of the quadratic polynomial with respect to k_B in the left part of Eq. (A9),

$$\frac{\gamma+2-\sqrt{\gamma^2+4}}{2}<\gamma+1<\frac{\gamma+2+\sqrt{\gamma^2+4}}{2}. \quad \text{(A10)}$$

Because of the condition $k_B<\gamma+1$ obtained above, there are two intervals for k_B. The first of these is $k_B\in((\gamma+2-\sqrt{\gamma^2+4})/2;\gamma+1)$. In this case, one has $[k_B^2-k_B(\gamma+2)+\gamma]<0$; thus, k_S must satisfy the condition $k_S>[k_B(k_B-2)]/[k_B^2-k_B(\gamma+2)+\gamma]$. However, this condition is in contradiction with the condition that follows from the requirement of the positivity of the second minor obtained above: $k_S<(k_B-1)/[k_B-(\gamma+1)]$. Therefore, k_B belongs to the second interval: $k_B\in(-\infty;(\gamma+2-\sqrt{\gamma^2+4})/2)$. In this case, k_S must satisfy the following condition: $k_S<[k_B(k_B-2)]/[k_B^2-k_B(\gamma+2)+\gamma]$. Note that this condition for k_S is more restrictive than the condition obtained from the requirement of the positivity of the second minor. Finally, in the case of $N=3$, the stability criterion of the perpendicular state can be written as

$$k_B<k_{B\,\max}^{\perp}(3)=\frac{\gamma+2-\sqrt{\gamma^2+4}}{2}<1,$$

$$k_S<k_{SC}^{\perp}(3)=\frac{k_B(k_B-2)}{k_B^2-(\gamma+2)k_B+\gamma}. \quad \text{(A11)}$$

This result is remarkable. First, $k_{B\,\max}^{\perp}(3)$ equals zero at $\gamma=0$, and if γ approaches infinity, $\gamma\to+\infty$, $k_{B\,\max}^{\perp}(3)$ monotonously increases up to 1. It means that for $k_B>1$, the perpendicular state cannot occur for any magnitude of $\gamma>0$. This result differs from the result obtained for $N=2$. Below, it will be shown that for any $N>2$, the parameter $k_{B\,\max}^{\perp}(N)$ is bounded from above. It is a general property of the stability criterion of the perpendicular state for arbitrary $N>2$. Second, $k_{B\,\max}^{\perp}(3)$ is determined by the minimal positive root of the polynomial in the denominator in Eq. (A11). This is characteristic of the stability criterion of the perpendicular state for any integer $N>2$.

$N=4$. Matrix $A_{4\times4}$ has the following form:

$$A_{4\times4}=\begin{Vmatrix} \frac{\gamma(1-k_S)}{2} & -\frac{\gamma}{2} & 0 & 0 \\ -\frac{\gamma}{2} & \frac{-k_B+\gamma+1}{2} & -\frac{1}{2} & 0 \\ 0 & -\frac{1}{2} & -\frac{k_B}{2}+1 & -\frac{1}{2} \\ 0 & 0 & -\frac{1}{2} & -\frac{k_B}{2}+\frac{1}{2} \end{Vmatrix}. \quad \text{(A12)}$$

This is the last particular case we consider because in contrast to $N=1$, 2, and 3 in all cases with $N\geqslant4$, the form of the matrix $A_{N\times N}$ is the same; i.e., it no longer depends on N. The requirements $d_1A>0$, $d_2A>0$ for matrix $A_{4\times4}$ give rise to the same conditions for k_S, k_B as in the case of $A_{3\times3}$. The requirement $d_3A>0$ for matrix $A_{4\times4}$ differs from the requirement $d_3A>0$ for matrix $A_{3\times3}$ and can be written as

$$k_S[k_B^2-k_B(\gamma+3)+2\gamma+1]<k_B^2-3k_B+1. \quad \text{(A13)}$$

A detailed consideration of the requirement $d_3A>0$ is crucial for the present investigation since matrices $A_{N\times N}$ are of the same form for any $N\geqslant4$. In other words, the conditions for k_S, k_B resulting from the requirement $d_3A>0$ are general and will be used below in order to derive a general formula for the stability criterion for any integer N. One can show that the parameter $(\gamma+1)$ is within the interval limited by the roots of the quadratic polynomial with respect to k_B in the left-hand side of Eq. (A13) for any $\gamma>0$,

$$\frac{\gamma+3-\sqrt{\gamma^2-2\gamma+5}}{2}<\gamma+1<\frac{\gamma+3+\sqrt{\gamma^2-2\gamma+5}}{2}. \quad \text{(A14)}$$

Since the requirement $d_2A>0$ for matrix $A_{4\times4}$ leads to the condition $k_B<\gamma+1$, there are two possible intervals for k_B. The first interval is $k_B\in((\gamma+3-\sqrt{\gamma^2+4})/2;\gamma+1)$. Then, the quadratic polynomial in the left-hand side of Eq. (A13) is negative and, thus, the following condition results from Eq. (A13)

$$k_S>\frac{k_B^2-3k_B+1}{k_B^2-k_B(\gamma+3)+2\gamma+1}. \quad \text{(A15)}$$

However, condition (A15) contradicts the condition for k_S obtained from the requirement $d_2A>0$ for matrix $A_{4\times4}$. Therefore, one has to conclude that k_B belongs to the interval: $k_B\in(-\infty;(\gamma+3-\sqrt{\gamma^2-2\gamma+5})/2)$; i.e., the quadratic polynomial in the left-hand side of Eq. (A13) is positive. If γ

approaches infinity, $\gamma \to +\infty$, then the upper border of this interval increases monotonously and approaches 2. Therefore, for $N \geqslant 4$ and $\gamma > 0$, the perpendicular state cannot occur for $k_B > 2$. In the considered case, the condition for k_S resulting from the requirement $d_3 A > 0$ can be written as

$$k_S < \frac{k_B^2 - 3k_B + 1}{k_B^2 - k_B(\gamma + 3) + 2\gamma + 1}. \tag{A16}$$

The requirement $d_4 A > 0$ for matrix $A_{4\times 4}$ can be written as

$$k_S[k_B(k_B^2 - 4k_B + 3) - \gamma(k_B^2 - 3k_B + 1)] > k_B(k_B^2 - 4k_B + 3). \tag{A17}$$

If the cubic polynomial with respect to k_B [in square brackets in the left-hand side of Eq. (A17)] is positive, then the condition for k_S, following from Eq. (A17), contradicts the condition for k_S following from the requirement $d_3 A > 0$ for matrix $A_{4\times 4}$. Therefore, we have to conclude that the cubic polynomial in the square brackets in Eq. (A17) is negative. Simple analyses of the inequality

$$k_B(k_B^2 - 4k_B + 3) - \gamma(k_B^2 - 3k_B + 1) < 0 \tag{A18}$$

taking account of the conditions for k_B, following from the requirement $d_3 A > 0$, show that the parameter k_B must be smaller than the minimal positive root of the cubic polynomial [Eq. (A18)]. We denote this root as $k_{B\,\max}^{\perp}(4)$. For $N = 4$, this is the most restrictive condition for k_B. Finally, in the case of $N = 4$, the stability criterion can be written as

$$k_B < k_{B\,\max}^{\perp}(4) < 2\left(1 - \cos\left(\frac{\pi}{5}\right)\right),$$

$$k_S < k_{SC}^{\perp}(4) = \frac{k_B(k_B^2 - 4k_B + 3)}{k_B(k_B^2 - 4k_B + 3) - \gamma(k_B^2 - 3k_B + 1)}. \tag{A19}$$

The expression for $k_{B\,\max}^{\perp}(4)$ in Eq. (A19) is not shown because it is too bulky.

The derivation of the stability criterion of the perpendicular state for particular $N = 2$, 3, and 4 [formulas (A7), (A11), and (A19)], based on the requirement of the positivity of all corner minors of the corresponding matrices [Eqs. (A5), (A8), and (A12)], reveals the following trends.

(1) In every case considered above, there is the condition $k_S < 1$ following from the requirement $d_1 A > 0$. This condition does not depend on the value of N.

(2) The form of the matrix that determines the expression for the minor $d_n A$ $(4 \leqslant n \leqslant N-1)$ does not change with the minor index. The requirement of the positivity of every next minor leads to a more restrictive condition from above for the parameters k_B and k_S.

(3) The form of the matrix that corresponds to the last minor $d_N A$ differs from that for every previous minor $d_n A$ $(2 \leqslant n \leqslant N-1)$. The most restrictive condition for k_B and k_S follows from the requirement of the positivity of the last minor $d_N A$.

(4) For each integer $N = 2$, 3, and 4 and $\gamma > 0$, the magnitude of $k_{B\,\max}^{\perp}(N)$ coincides with the minimal positive root of the function in the denominator of the expression for $k_{SC}^{\perp}(N)$.

It turns out that these statements are valid for all integer N rather than only for $N = 2$, 3, and 4. The first statement is obvious. All the other statements can be proven using the method of mathematical induction.

In terms of the model parameter k_B, a laconic formulation of the stability criterion of the perpendicular state is impossible. However, the analytic form of this criterion can be written in terms of determinants of the square $(n \times n)$ three-diagonal matrix $C_{ij} = \varepsilon \delta_{ij} - \frac{1}{2}\delta_{ij+1} - \frac{1}{2}\delta_{ij-1}$,

$$C_{ij} = \begin{Vmatrix} \varepsilon & -\frac{1}{2} & 0 & \ldots & 0 & 0 & 0 \\ -\frac{1}{2} & \varepsilon & -\frac{1}{2} & 0 & \ldots & 0 & 0 \\ 0 & -\frac{1}{2} & \varepsilon & \ldots & \ldots & \ldots & 0 \\ \ldots & 0 & \ldots & \ldots & \ldots & 0 & \ldots \\ 0 & \ldots & \ldots & \ldots & \varepsilon & -\frac{1}{2} & 0 \\ 0 & 0 & \ldots & 0 & -\frac{1}{2} & \varepsilon & -\frac{1}{2} \\ 0 & 0 & 0 & \ldots & 0 & -\frac{1}{2} & \varepsilon \end{Vmatrix}. \tag{A20}$$

For various values of the parameter ε, the determinant of this matrix has different forms,

$$\det C_{n\times n} = \begin{cases} \dfrac{\sinh \varphi(n+1)}{2^n \sinh \varphi}, & \varepsilon > 1, \quad \varepsilon = \cosh \varphi, \quad \varphi > 0 \\ \dfrac{\sin \varphi(n+1)}{2^n \sin \varphi}, & -1 \leqslant \varepsilon \leqslant 1, \quad \varepsilon = \cos \varphi, \quad 0 \leqslant \varphi \leqslant \pi \\ (-1)^n \dfrac{\sinh \varphi(n+1)}{2^n \sinh \varphi}, & \varepsilon < -1, \quad \varepsilon = -\cosh \varphi, \quad \varphi > 0. \end{cases} \tag{A21}$$

For matrix $A_{N\times N}$ [Eq. (A2)], ε is determined by the expression $\varepsilon=-k_B/2+1$. This means that varying the model parameter k_B, we have to consider all possible cases.

(1) $-k_B/2+1<-1\Rightarrow k_B>4$. The derivation of the stability criterion for $N=2$, 3, and 4 has shown that for $N\geqslant 2$ the perpendicular state cannot occur for $k_B>2$. Therefore, this case can be ignored.

(2) $-1\leqslant -k_B/2+1\leqslant +1\Rightarrow 0\leqslant k_B\leqslant 4$. Because of the restriction $k_B<2$ mentioned above, it makes sense to consider this case only within the interval $0\leqslant k_B<2$. This corresponds to the experimental situation related to Co/Au films where the bulk anisotropy constant favors the in-plane state. In accordance with the expression for the model thermodynamic potential, Eq. (3), the in-plane state is realized for positive bulk anisotropy constant k_B.

(3) $-k_B/2+1>+1\Rightarrow k_B<0$. In the present work, we search for the stability criterion of the perpendicular state for arbitrary anisotropy constants k_S and k_B rather than only for those that correspond to the magnetic properties of Co/Au films. Therefore, this case needs to be considered to be able to construct the general diagram of magnetic states of a film with arbitrary k_S and k_B.

In accordance with what was said above, the stability criterion of the perpendicular state for $k_B>0$ can be written as

$$0\leqslant k_B<k_{B\,\max}(N)\equiv 2(1-\cos\varphi^*),\quad \varphi(k_B)=\arccos\left(-\frac{k_B}{2}+1\right),$$

$$k_S\leqslant k_{SC}^{\perp}(N)\equiv\frac{\sin\varphi N-2\sin\varphi(N-1)+\sin\varphi(N-2)}{\sin\varphi N-\sin\varphi(N-1)+(\gamma-1)[\sin\varphi(N-1)-\sin\varphi(N-2)]}. \tag{A22}$$

Here, φ^* is a minimal root of the equation in the interval $(0,\pi)$,

$$\sin\varphi N-\sin\varphi(N-1)+(\gamma-1)[\sin\varphi(N-1)-\sin\varphi(N-2)]=0. \tag{A23}$$

In the particular case $\gamma=1$, the expression for $k_{B\,\max}^{\perp}(N)$ can be obtained in a closed form,

$$\gamma=1,\quad k_{B\,\max}^{\perp}(N)=2\left[1-\cos\left(\frac{\pi}{2N-1}\right)\right]. \tag{A24}$$

In a more general case of $\gamma\neq 1$, one can get the estimate for $k_{B\,\max}^{\perp}(N)$ from above. This estimate appears to be very useful for plotting the diagram of magnetic states in coordinates (γ,k_S,k_B) for arbitrary N,

$$k_{B\,\max}^{\perp}(N)<2\left[1-\cos\left(\frac{\pi}{2N-3}\right)\right]. \tag{A25}$$

It follows from Eq. (A22) that $k_{SC}^{\perp}(N)<0$, $k_{B\,\max}^{\perp}(N+1)<k_{B\,\max}^{\perp}(N)$, $k_{SC}^{\perp}(N+1)<k_{SC}^{\perp}(N)$, and $\lim_{N\to\infty}k_{B\,\max}^{\perp}(N)=0$. This means that for $k_B\geqslant 0$, the region corresponding to the perpendicular state in the (k_S,k_B) diagram is situated in the left part of the diagram $(k_S<0)$. This region decreases monotonously with film thickness N, and in the limiting case $N\to\infty$ it totally disappears. Therefore, for $k_B\geqslant 0$, the existence of the perpendicular state is entirely determined by the finite thickness of the film.

For $k_B<0$, the stability criterion of the perpendicular state of an N-layer film is the following:

$$k_S<k_{SC}^{\perp}(N)\equiv\frac{\sinh\varphi N-2\sinh\varphi(N-1)+\sinh\varphi(N-2)}{\sinh\varphi N-\sinh\varphi(N-1)+(\gamma-1)[\sinh\varphi(N-1)-\sinh\varphi(N-2)]},$$

$$\varphi(k_B)=\ln\left[\left(-\frac{k_B}{2}+1\right)+\sqrt{\left(-\frac{k_B}{2}+1\right)^2-1}\right],\quad k_B<0. \tag{A26}$$

′It follows from Eq. (A26) that $0<k_{SC}^{\perp}(N)<1$, $k_{SC}^{\perp}(N+1)<k_{SC}^{\perp}(N)$, and $\lim_{N\to\infty}k_{SC}^{\perp}(N)<1$. This means that for $k_B<0$ the region corresponding to the perpendicular state in the diagram of magnetic states is confined to the right-hand side by the curve determined by the function $k_S=k_{SC}^{\perp}(N,k_B)$. As the film thickness increases, the right border of this region shifts to the right. In the limiting case $N\to\infty$, the right border approaches the position that corresponds to the perpendicular-canted noncollinear border for the semi-infinite sample $k_{SC}^{\perp}(N\to\infty,k_B)<1$.

It can be shown that the substitution of φ by the expressions for $\varphi(k_B)$, defined by Eqs. (A22) and (A26), in the corresponding formulas for $k_{SC}^{\perp}(N)$ [Eqs. (A22) and (A26)] for a particular N leads to the same expression for $k_{SC}^{\perp}(N)$ regardless of which formula, Eq. (A22) or (A26), is used. This is not a surprising result because no matter what kind of parametrization is applied, $\cos\varphi=-k_B/2+1$ or $\cosh\varphi=-k_B/2+1$ in both cases, one uses the same matrix [Eq. (A2)].

Naturally, the analytic expressions for the stability criterion of the perpendicular state [the dependence of $k_{SC}^{\perp}(N)$ on k_B], following from Eq. (A22) or (A26), for $N=2$, 3, and 4, coincide with the results obtained above for the particular cases [formulas (A7), (A11), and (A19)]. To simplify the construction of the diagram of magnetic states, one should use the explicit expression for the dependence of $k_{SC}^{\perp}(N,k_B)$ on k_B. Since for large N these formulas are too bulky, we write them in the following way:

$$k_B < k_{B\,\max}^{\perp}(N) < 2\left[1-\cos\left(\frac{\pi}{2N-3}\right)\right], \tag{A27}$$

$$k_S \leqslant k_{SC}^{\perp}(N,k_B) \equiv \frac{P_{N-1}(k_B)+P_{N-2}(k_B)}{P_{N-1}(k_B)-(\gamma-1)P_{N-2}(k_B)}. \tag{A28}$$

Here, $k_{B\,\max}^{\perp}(N)$ is a minimal positive root of the equation

$$P_{N-1}(k_B)-(\gamma-1)P_{N-2}(k_B)=0. \tag{A29}$$

For $\gamma>0$, Eq. (A29) has $N-1$ real positive roots $k_{B1},k_{B2},\ldots,k_{B(N-1)}$. Note that in the present work, we always show the diagram of magnetic states in coordinates (k_S,k_B). Because of that, these roots determine the position of the $N-1$ horizontal asymptotes in the plot of $k_{SC}^{\perp}(N,k_B)$ (horizontal axis) versus k_B (vertical axis) [Eq. (A28)], and this plot contains N curves separated from each other by $(N-1)$ horizontal asymptotes. In the (k_S,k_B) plane, the border of the region of the stability of the perpendicular state is determined by the lowest curve situated below the lowest horizontal asymptote. The position of this asymptote is determined by the right-hand side of the inequality [Eq. (A27)]. All the other $N-1$ curves in the plot of $k_{SC}^{\perp}(N,k_B)$ versus k_B are irrelevant.

The polynomials $P_i(k_B)$ necessary to obtain the dependence of $k_{SC}^{\perp}(N,k_B)$ on k_B for $N=2,3,\ldots,10$ [Eq. (A28)] are defined below,

$$P_0(k_B)=1,$$

$$P_1(k_B)=k_B-1,$$

$$P_2(k_B)=k_B^2-3k_B+1,$$

$$P_3(k_B)=k_B^3-5k_B^2+6k_B-1,$$

$$P_4(k_B)=k_B^4-7k_B^3+15k_B^2-10k_B+1,$$

$$P_5(k_B)=k_B^5-9k_B^4+28k_B^3-35k_B^2+15k_B-1,$$

$$P_6(k_B)=k_B^6-11k_B^5+45k_B^4-84k_B^3+70k_B^2-21k_B+1,$$

$$P_7(k_B)=k_B^7-13k_B^6+66k_B^5-165k_B^4+210k_B^3-126k_B^2+28k_B-1,$$

$$P_8(k_B)=k_B^8-15k_B^7+91k_B^6-286k_B^5+495k_B^4-462k_B^3+210k_B^2-36k_B+1,$$

$$P_9(k_B)=k_B^9-17k_B^8+120k_B^7-455k_B^6+1001k_B^5-1287k_B^4+924k_B^3-330k_B^2+45k_B-1. \tag{A30}$$

APPENDIX B: STABILITY CRITERION OF THE IN-PLANE STATE OF A FILM OF FINITE THICKNESS

The stability conditions for the in-plane state of a ferromagnetic film corresponding to the minimal magnitude of the thermodynamic potential [Eq. (3)] can be found using the same approach as the one described in Appendix A, i.e., the approach based on the Silvestre criterion. One should expand the thermodynamic potential [Eq. (3)] to the second order of θ_n in the vicinity of the point $\theta_n=0$, $n=1,2,3,\ldots,N$. In this expansion, the terms of the first order of θ_n are absent because at the point $\theta_n=0$, $n=1,2,3,\ldots,N$, the thermodynamic potential is minimal, i.e., the first derivative of thermodynamic potential with respect to every θ_n equals zero. Then, one should find the necessary and sufficient conditions for the quadratic form

$$\Delta\varphi=\vec{\theta}^T\hat{B}\vec{\theta} \tag{B1}$$

to be positive. Here, $\vec{\theta}=(\theta_1,\theta_2,\theta_3,\ldots,\theta_N)$, $\Delta\varphi$ is an increment in the thermodynamic potential [Eq. (3)] caused by a deviation of the orientation angles θ_n from zero. The operator $\hat{B}$ in Eq. (B1) corresponds to a square $(N\times N)$ three-diagonal symmetric matrix with real matrix elements

$$B_{N\times N}=\begin{Vmatrix} \frac{\gamma(1+k_S)}{2} & -\frac{\gamma}{2} & 0 & 0 & \cdots & 0 & 0 & 0 \\ -\frac{\gamma}{2} & \frac{+k_B+\gamma+1}{2} & -\frac{1}{2} & 0 & \cdots & 0 & 0 & 0 \\ 0 & -\frac{1}{2} & \frac{k_B}{2}+1 & -\frac{1}{2} & \cdots & 0 & 0 & 0 \\ 0 & 0 & -\frac{1}{2} & \frac{k_B}{2}+1 & \cdots & \cdots & \cdots & \cdots \\ \cdots & \cdots & \cdots & \cdots & \cdots & \cdots & \cdots & \cdots \\ 0 & 0 & 0 & 0 & \cdots & \frac{k_B}{2}+1 & -\frac{1}{2} & 0 \\ 0 & 0 & 0 & 0 & \cdots & -\frac{1}{2} & \frac{k_B}{2}+1 & -\frac{1}{2} \\ 0 & 0 & 0 & 0 & \cdots & 0 & -\frac{1}{2} & \frac{k_B}{2}+\frac{1}{2} \end{Vmatrix}. \tag{B2}$$

The comparison of matrix $B_{N\times N}$ [Eq. (B2)] with matrix $A_{N\times N}$ [Eq. (A2)] (Appendix A) shows that these matrices have a similar form with the only difference that in matrix $B_{N\times N}$ all the anisotropy constants have the opposite sign. Therefore, the stability criterion of the in-plane state can be obtained from that for perpendicular state just by changing signs of k_S and k_B.

For negative k_B, the stability criterion for a N-layer film can be written as

$$0 \geqslant k_B > k_{B\,\min}^{\parallel}(N) \equiv -2(1-\cos\varphi^*) > -2\left[1-\cos\left(\frac{\pi}{2N-3}\right)\right], \quad \varphi(k_B)=\arccos\left(\frac{k_B}{2}+1\right),$$

$$k_S \geqslant k_{SC}^{\parallel}(N) \equiv -\frac{\sin\varphi N-2\sin\varphi(N-1)+\sin\varphi(N-2)}{\sin\varphi N-\sin\varphi(N-1)+(\gamma-1)[\sin\varphi(N-1)-\sin\varphi(N-2)]}. \tag{B3}$$

Here, φ^* is a minimal positive root of the equation

$$\sin\varphi N-\sin\varphi(N-1)+(\gamma-1)[\sin\varphi(N-1)-\sin\varphi(N-2)]=0 \tag{B4}$$

in the interval $(0,\pi)$. It follows from Eq. (B3) that for $k_B \leqslant 0$ there is a minimal value of bulk anisotropy constant $k_{B\,\min}^{\parallel}(N) < 0$. If $k_B < k_{B\,\min}^{\parallel}(N) < 0$, the in-plane state cannot exist for any positive k_S. It can be shown that $k_{SC}^{\parallel}(N) > 0$, $k_{B\,\min}^{\parallel}(N+1) > k_{B\,\min}^{\parallel}(N)$, $k_{SC}^{\parallel}(N+1) > k_{SC}^{\parallel}(N)$, and $\lim_{N\to\infty} k_{B\,\min}^{\parallel}(N)=0$. This means that for $k_B \leqslant 0$, the region corresponding to the in-plane state in the (k_S,k_B) diagram is situated in the right part of the diagram $(k_S>0)$. It decreases monotonously with thickness N, and in the limiting case, $N\to\infty$ totally disappears. Therefore, the existence of the in-plane state for $k_B \leqslant 0$ is entirely determined by the finite thickness of the film.

For the positive values of k_B, the stability criterion of the in-plane state of an N-layer film can be written as

$$k_S > k_{SC}^{\parallel}(N) \equiv -\frac{\sinh\varphi N-2\sinh\varphi(N-1)+\sinh\varphi(N-2)}{\sinh\varphi N-\sinh\varphi(N-1)+(\gamma-1)[\sinh\varphi(N-1)-\sinh\varphi(N-2)]},$$

$$\varphi(k_B)=\ln\left[\left(\frac{k_B}{2}+1\right)+\sqrt{\left(\frac{k_B}{2}+1\right)^2-1}\right], \quad k_B>0. \tag{B5}$$

It follows from Eq. (B5) that for $k_B>0$, one has $-1 < k_{SC}^{\parallel}(N) < 0$, $k_{SC}^{\parallel}(N+1) > k_{SC}^{\parallel}(N)$, and $\lim_{N\to\infty} k_{SC}^{\parallel}(N) = -1+\gamma/(e^{\varphi}-1+\gamma)$. This means that for $k_B>0$, the region corresponding to the in-plane state in the diagram of magnetic states is confined only from the left-hand side by the curve determined by the negative function $k_S \equiv k_{SC}^{\parallel}(N,k_B)$. This region expands to the left with film thickness. In the limiting case $N\to\infty$, the left border of this region approaches the border between the in-plane and canted noncollinear regions for a semi-infinite sample.

It can be shown that for particular N, the substitution of φ in Eqs. (B3) and (B5) with the expression for $\varphi(k_B)$ leads to

the same expression for $k_{SC}^{\parallel}(N)$ regardless of what formula is used, Eq. (B3) or (B5). This is not surprising because no matter what kind of parametrization is applied in both cases, one uses the same matrix [Eq. (B2)].

For $N=2$, the stability criterion of the in-plane state can be written as

$$k_B > -\gamma,$$

$$k_S > k_{SC}^{\parallel}(2) \equiv -\frac{k_B}{k_B+\gamma}. \tag{B6}$$

For $N=3$, the stability criterion can be written as

$$k_B > k_{B\,\min}^{\parallel}(3) \equiv -\frac{\gamma+2-\sqrt{\gamma^2+4}}{2} > -1,$$

$$k_S > k_{SC}^{\parallel}(3) \equiv -\frac{k_B(k_B+2)}{k_B^2+(\gamma+2)k_B+\gamma}. \tag{B7}$$

For $N=4$, the criterion can be written as

$$k_B > k_{B\,\min}^{\parallel}(4) > -2\left(1-\cos\left(\frac{\pi}{5}\right)\right),$$

$$k_S > k_{SC}^{\parallel}(4) \equiv -\frac{k_B(k_B^2+4k_B+3)}{k_B(k_B^2+4k_B+3)+\gamma(k_B^2+3k_B+1)}. \tag{B8}$$

The expression for $k_{B\,\min}^{\parallel}(4)$ in Eq. (B8) is not shown because it is too bulky. $k_{B\,\min}^{\parallel}(4)$ is a maximal negative root of the polynomial in the denominator of the expression for $k_{SC}^{\parallel}(4)$.

It follows from Eq. (B7) and (B8) as well as from the requirement of the positivity of the third minor of matrix $B_{4\times4}$ that for $N>2$ the in-plane state cannot occur for the bulk anisotropy constant $k_B<-2$.

To simplify the construction of the diagram of magnetic states for an arbitrary N, one should use the explicit expression for the dependence of $k_{SC}^{\parallel}(N,k_B)$ on k_B. Since this expression is too bulky for large N, we write it in the following form:

$$k_B > k_{B\,\min}^{\parallel}(N,\gamma) > -2\left[1-\cos\left(\frac{\pi}{2N-3}\right)\right], \tag{B9}$$

$$k_S \geqslant k_{SC}^{\parallel}(N,k_B) \equiv -\frac{Q_{N-1}(k_B)-Q_{N-2}(k_B)}{Q_{N-1}(k_B)+(\gamma-1)Q_{N-2}(k_B)}. \tag{B10}$$

Here, $k_{B\,\min}^{\parallel}(N,\gamma)$ is a maximal negative root of the equation

$$Q_{N-1}(k_B)+(\gamma-1)Q_{N-2}(k_B)=0. \tag{B11}$$

The polynomials $Q_i(k_B)$ necessary for obtaining the expression $k_{SC}^{\parallel}(N,k_B)$ for $N=2,3,\ldots,10$ [Eq. (B10)] are defined below,

$$Q_0(k_B)=1,$$

$$Q_1(k_B)=k_B+1,$$

$$Q_2(k_B)=k_B^2+3k_B+1,$$

$$Q_3(k_B)=k_B^3+5k_B^2+6k_B+1,$$

$$Q_4(k_B)=k_B^4+7k_B^3+15k_B^2+10k_B+1,$$

$$Q_5(k_B)=k_B^5+9k_B^4+28k_B^3+35k_B^2+15k_B+1,$$

$$Q_6(k_B)=k_B^6+11k_B^5+45k_B^4+84k_B^3+70k_B^2+21k_B+1,$$

$$Q_7(k_B)=k_B^7+13k_B^6+66k_B^5+165k_B^4+210k_B^3+126k_B^2+28k_B+1,$$

$$Q_8(k_B)=k_B^8+15k_B^7+91k_B^6+286k_B^5+495k_B^4+462k_B^3+210k_B^2+36k_B+1,$$

$$Q_9(k_B)=k_B^9+17k_B^8+120k_B^7+455k_B^6+1001k_B^5+1287k_B^4+924k_B^3+330k_B^2+45k_B+1. \tag{B12}$$

[1] H. E. Stanley, *Introduction to Phase Transitions and Critical Phenomena* (Oxford University Press, Oxford, 1971).

[2] L. M. Falicov, D. T. Pierce, S. D. Bader, R. Gronsky, K. B. Hathaway, H. J. Hopster, D. N. Lambeth, S. S. P. Parkin, G. Prinz, M. Salamon, I. K. Schuller, and R. H. Victora, J. Mater. Res. **5**, 1990 (1990).

[3] D. Weller and A. Moser, IEEE Trans. Magn. **35**, 4423 (1999).

[4] J. A. C. Bland and B. Heinrich, *Ultrathin Magnetic Structures* (Springer, Berlin, 1994), Vols. I and II.

[5] P. J. Jensen and K. H. Bennemann, *Frontiers in Magnetic Materials*, edited by A. V. Narlikar (Springer, Berlin, 2005).

[6] P. J. Jensen and K. H. Bennemann, Surf. Sci. Rep. **61**, 129 (2006).

[7] C. Liu, E. R. Moog, and S. D. Bader, Phys. Rev. Lett. **60**, 2422 (1988).

[8] D. P. Pappas, K. P. Kamper, and H. Hopster, Phys. Rev. Lett. **64**, 3179 (1990).

[9] N. C. Koon, B. T. Jonker, F. A. Volkening, J. J. Krebs, and G. A. Prinz, Phys. Rev. Lett. **59**, 2463 (1987).

[10] D. P. Pappas, C. R. Brundle, and H. Hopster, Phys. Rev. B **45**, 8169 (1992).

[11] Z. Q. Qiu, J. Pearson, and S. D. Bader, Phys. Rev. Lett. **70**, 1006 (1993).

[12] A. Berger and H. Hopster, Phys. Rev. Lett. **76**, 519 (1996).

[13] R. Allenspach, M. Stampanoni, and A. Bischof, Phys. Rev. Lett. **65**, 3344 (1990).

[14] J. Pommier, P. Meyer, G. Penissard, J. Ferre, P. Bruno, and D. Renard, Phys. Rev. Lett. **65**, 2054 (1990).

[15] M. Speckmann, H. P. Oepen, and H. Ibach, Phys. Rev. Lett. **75**, 2035 (1995).
[16] H. F. Ding, S. Putter, H. P. Oepen, and J. Kirschner, Phys. Rev. B **63**, 134425 (2001).
[17] S. Putter, H. F. Ding, Y. T. Millev, H. P. Oepen, and J. Kirschner, Phys. Rev. B **64**, 092409 (2001).
[18] R. Sellmann, H. Fritzsche, H. Maletta, V. Leiner, and R. Seibrecht, Phys. Rev. B **64**, 054418 (2001).
[19] W. L. O'Brien and B. P. Tonner, Phys. Rev. B **49**, 15370 (1994).
[20] B. Schulz and K. Baberschke, Phys. Rev. B **50**, 13467 (1994).
[21] W. L. O'Brien, T. Droubay, and B. P. Tonner, Phys. Rev. B **54**, 9297 (1996).
[22] L. Neel, J. Phys. Radium **15**, 225 (1954).
[23] J. I. Hong, S. Sankar, A. E. Berkowitz, and W. F. Egelhoff, Jr., J. Magn. Magn. Mater. **285**, 359 (2005).
[24] R. Allenspach (private communication).
[25] L. D. Landau and E. M. Lifshitz, *Electrodynamics of Continuous Media* (Pergamon, Oxford, 1960), Chap. 5.
[26] L. Udvardi, R. Kiraly, L. Szunyogh, F. Denat, M. B. Taylor, B. L. Gyorffy, B. Ujfalussy, and C. Uiberacker, J. Magn. Magn. Mater. **183**, 283 (1998).
[27] L. Udvardi, L. Szunyogh, A. Vernez, and P. Weinberger, Philos. Mag. B **81**, 613 (2001).
[28] D. Jiles, *Introduction to Magnetism and Magnetic Meterials* (Chapman and Hall, London, 1991), p. 134.
[29] D. L. Mills, Phys. Rev. B **39**, 12306 (1989).
[30] R. P. Erickson and D. L. Mills, Phys. Rev. B **43**, 10715 (1991).
[31] A. Thiaville and A. Fert, J. Magn. Magn. Mater. **113**, 161 (1992).
[32] Xiao Hu and Yoshiyuki Kawazoe, Phys. Rev. B **51**, 311 (1995).
[33] Xiao Hu, Ruibao Tao, and Yoshiyuki Kawazoe, Phys. Rev. B **54**, 65 (1996).
[34] Xiao Hu, Phys. Rev. B **55**, 8382 (1997).
[35] A. P. Popov and D. P. Pappas, Phys. Rev. B **64**, 184401 (2001).
[36] K. D. Usadel and A. Hucht, Phys. Rev. B **66**, 024419 (2002).
[37] L. Szunyogh (private communication).
[38] L. Szunyogh, B. Ujfalussy, and P. Weinberger, Phys. Rev. B **51**, 9552 (1995).
[39] B. Ujfalussy, L. Szunyogh, and P. Weinberger, Phys. Rev. B **54**, 9883 (1996).
[40] Y. Yafet and E. M. Gyorgy, Phys. Rev. B **38**, 9145 (1988).
[41] R. Czech and J. Villain, J. Phys.: Condens. Matter **1**, 619 (1989).
[42] A. B. Kashuba and V. L. Pokrovsky, Phys. Rev. Lett. **70**, 3155 (1993).
[43] A. B. Kashuba and V. L. Pokrovsky, Phys. Rev. B **48**, 10335 (1993).
[44] P. J. Jensen and K. H. Bennemann, Phys. Rev. B **52**, 16012 (1995).
[45] B. Kaplan and G. A. Gehring, J. Magn. Magn. Mater. **128**, 111 (1999).
[46] M. G. Pini, A. Rettori, D. P. Pappas, A. V. Anisimov, and A. P. Popov, J. Magn. Magn. Mater. **272-276**, 1152 (2004).
[47] A. P. Popov, A. V. Anisimov, and D. P. Pappas, Phys. Rev. B **67**, 094428 (2003).
[48] C. S. Arnold, D. P. Pappas, and A. P. Popov, Phys. Rev. Lett. **83**, 3305 (1999).
[49] C. R. Arnold, D. P. Pappas, and A. P. Popov, J. Appl. Phys. **87**, 5478 (2000).
[50] A. V. Anisimov and A. P. Popov, JETP **101**, 830 (2005).
[51] A. Taga, L. Nordström, P. James, B. Johansson, and O. Eriksson, Nature (London) **406**, 280 (2000).